fluids

MDPI

Article

Effects of Channelling a Peripherally Inserted Central Venous Catheter on Blood Flow

Laura Hernández-Cabré [1,2], Marta Ulldemolins-Rams [1], Judit Vilanova-Corsellas [3,4] and Carles Torras [1,5,*]

[1] Institut Julio Antonio, Móra d'Ebre, 43740 Tarragona, Spain; lhernandez@iesjulioantonio.cat or laura.hernandez.cabre@gmail.com (L.H.-C.); mulldemolins@iesjulioantonio.cat or martaullra@gmail.com (M.U.-R.)
[2] School of Engineering, Universitat Rovira i Virgili, 43007 Tarragona, Spain
[3] Servicio de Medicina Intensiva, Hospital Universitari Arnau de Vilanova de Lleida, 25198 Lleida, Spain; jvilanova.lleida.ics@gencat.cat or judvilanova@gmail.com
[4] Department of Medicine and Surgery, Universitat de Lleida, 25198 Lleida, Spain
[5] Department of Chemical Engineering, Universitat Rovira i Virgili, 43007 Tarragona, Spain
* Correspondence: carles.torras@urv.cat or ctorras7@xtec.cat or carlestorrasfont@gmail.com

Abstract: A catheter is a device that is inserted into the venous system to infuse treatment with controlled doses per unit of time. The study of its interaction with blood flow cannot be easily analysed with common analytical methods or different visualization techniques in real life. Computational Fluid Dynamics has become a very useful tool in a wide variety of fields of scientific study and has allowed access to the understanding of the anatomical and physiological functioning of the human body. In this work, Computational Fluid Dynamics is used to study the effects of inserting a catheter on blood flow and the quality of the mixture of blood with the various substances infused through this device. Results show that the insertion of the catheter not only does not worsen the blood circulation but improves it by reducing stagnant zones. Regarding mixture, a homogenization of the fluids in the venous area before their entrance to the heart was observed. Highest quality mixtures correspond to fewer infused fluids and at lower velocity.

Keywords: peripherally inserted central venous catheter; vein; blood; drugs; flow; mixture; computational fluid dynamics

Citation: Hernández-Cabré, L.; Ulldemolins-Rams, M.; Vilanova-Corsellas, J.; Torras, C. Effects of Channelling a Peripherally Inserted Central Venous Catheter on Blood Flow. *Fluids* **2024**, *9*, 245. https://doi.org/10.3390/fluids9110245

Academic Editors: Mehrdad Massoudi, D. Andrew S. Rees and Chengcheng Tao

Received: 25 July 2024
Revised: 11 October 2024
Accepted: 15 October 2024
Published: 22 October 2024

1. Introduction

The circulatory system aims to transport oxygen, nutrients and hormones to cells, and waste products such as carbon dioxide to the organs responsible for their excretion. It is made up of three main organs: blood, heart, and blood vessels [1]. Blood vessels are the ducts that carry blood throughout the body. They form a network of veins, arteries, arterioles, venulae and capillaries and have different functions in the circulatory system [2]. Blood vessels are divided into three types: arteries, veins and capillaries. The arteries are responsible for the distribution of oxygenated blood from the heart to the capillaries of the body. This blood is under high pressure, therefore the vascular walls of the arteries are strong to resist the pressure of the flow they transport. The veins return poorly oxygenated blood from the blood capillaries to the heart to be recycled back to the lungs for re-oxygenation. Veins usually surround an artery in a branched and irregular network. Finally, capillaries facilitate the exchange of oxygen, nutrients and waste between major blood vessels and organs and tissues [3]. The veins, unlike the arteries, are more abundant, their walls are thinner, their lumens larger and there is less smooth muscle and elastic tissue. The blood runs through the veins in increasing order of diameter, that is, from the smallest vessels to the vena cava, that sheds fluid into the heart and is the thickest vein. The blood has a laminar flow and its average velocity is 0.24 m/s. Its density ranges from 1.055 to 1.064 g/cm^3 in men and from 1.050 to 1.056 g/cm^3 in women [4]. It has a viscosity between 3.5 and 5.5 cP. The pH of blood is 7.4 in arteries and 7.35 in veins [5].

An intravenous catheter is a device consisting of a thin, flexible tube that is inserted into a vein for therapeutic purposes. It is used to infuse fluids, hemoderivatives, chemotherapy and other intravenous drugs. These catheters, depending on the blood vessel being channelled, can be of two types: central venous catheter of peripheral or central insertion [6]. Peripherally Inserted Central Catheters (PICCs) are used with veins of the upper extremities (cephalic, basilic and/or axillary veins). These catheters enter the superior vena cava through the blood vessels [7]. It should be borne in mind that catheters with a higher number of lumens are associated with an increased risk of infection. However, PICCs, which are the most used catheters, vary from 1 to 3 lumens of differing lengths that perform their function at different points in the vein [8,9]:

- The distal lumen is closest to the heart. It is used to inject fluid therapy and sedation, since, as its size is thick, it allows the flow of high volumes and viscous solutions.
- The medial lumen is usually used exclusively for parenteral nutrition. This should always be infused by a single lumen due to the risk of bacterial colonization. If parenteral nutrition is not to be administered, the medial lumen may be used for other treatments.
- The proximal lumen is the farthest from the heart and is used for inotropic drugs.
- Central venous catheters may be located at the level of the subclavian, jugular and/or femoral vein. This type of catheter carries a higher risk of thrombosis or bacterial infections [10]. There will be a brief description of tunnelled central catheters that are used as long-lasting catheters in chronic patients (oncological, nephropathic, etc.).

Doppler ultrasound is based on the fact that the frequency of sound changes when the emitter and/or receiver move. It is used to evaluate blood flow by measuring the movement of red blood cells, allowing us to obtain information regarding vascular permeability, flow direction, presence of stenosis, distal vascular resistance and vascularization of lesions [11]. In a Doppler study, many factors arise that limit the accuracy of the ultrasound. One important factor that affects the results obtained is venous distensibility; because of the vein's anatomy, when inserting a device inside (such as a catheter), it may dilate. On the other hand, due to this anatomical feature, the presence of the ultrasound scanner (which applies pressure on the blood vessel) has effects on the theoretically circular shape and, therefore, causes interference in the measurement of the vessel's diameter.

CFD is a methodology that mathematically predicts the flow of physical fluids using computational tools. It solves the equations derived from the fundamental laws of conservation of the physical properties of fluids. Laminar flow is the type of movement of a fluid when it is perfectly ordered and stratified, so that the fluid moves in parallel layers without mixing. Turbulent flow occurs when movement becomes more irregular, chaotic and unpredictable, the particles move in a disorderly manner and the trajectories of the particles form small and aperiodic vorticities [12]. The Reynolds number is the relationship between the inertia forces and the viscous forces of a fluid. It is a dimensionless parameter used to classify fluid systems in which viscosity is considered. If the Reynolds number is less than or equal to approximately 2000, this indicates laminar flow, and a higher Reynolds number indicates turbulent flow [13]. The Reynolds number is computed by using Equation (1).

$$Re = \frac{\rho \cdot v \cdot d}{\mu} \tag{1}$$

where ρ (kg·m^{-3}) is density, v (m/s) is velocity, d (m) is diameter and μ (Pa·s) is dynamic viscosity (in international system units).

Once the flow has been defined, the CFD simulator solves the problem by considering the conservation of mass (continuity equation, Equation (2)) and conservation of momentum (Navier-Stokes, Equation (3)).

$$\frac{\partial \rho}{\partial t} + \nabla \cdot \rho \vec{V} = 0 \tag{2}$$

$$\rho \frac{D\vec{V}}{Dt} = -\nabla p + \mu \nabla^2 \vec{V} + \rho \cdot \vec{g} \quad (3)$$

in which ρ (kg·m^{-3}) is density, t (s) is time, $\vec{V}$ (m·s^{-1}) is fluid velocity, $\vec{g}$ (m·s^{-2}) is gravity, μ (Pa·s) is dynamic viscosity, p (Pa) is pressure (in international system units), D is the differential operator and ∇ is the vector operator defined as Equation (4) shows (in rectangular coordinates):

$$\nabla = \vec{i}\frac{\partial}{\partial x} + \vec{j}\frac{\partial}{\partial y} + \vec{k}\frac{\partial}{\partial z} \quad (4)$$

An incompressible fluid flowing through a pipe at a given flow rate increases its velocity proportionally by the reduction of the cross-section area. The same amount of fluid must pass through any point in the tube in a certain time to ensure the continuity of flow [14].

Traditionally, the only way to optimize a design was by performing physical testing on product prototypes. However, once a more difficult geometry is encountered, the scope of analytical solutions to fundamental equations of fluid mechanics is limited and a numerical method to obtain a solution is chosen. With the rise of computers and increasing computational power, the field of CFD has become a common application tool for predicting real-world physics. Modern problems of fluid mechanics would be unfeasible to solve without the use of numerical methods [15].

Currently, CFD tools are used in a wide variety of experimental fields. In the medical field, CFD methodology has been in use for several decades. Early studies in 1998 considered two-dimensional systems to check the flow disturbance caused by an intravascular catheter [16]. From then, a variety of papers were published, addressing the relationship between arteries and veins and inserted devices in 3D models, for example [17–19]. Two interesting studies in 3D refer to the effects of different angles of insertion of the catheter [20,21]. The modelling of the veins and arteries is a complex task due to the non-regular structure of the cavities, the variation between individuals and the flexibility of the vessels. Recent research using CFD also addresses these issues. Some examples are studies regarding carotid artery blood flow to compare models with rigid and elastic walls using CFD tools [22,23] or transient simulations of the bloodstream within a cerebral aneurysm to reveal the impacts of blood velocity on the risk of aneurysm rupture [24].

Using CFD methodology to simulate blood flow presents some challenges due to the nature of the blood. Blood is a complex fluid mainly composed of white blood cells, red blood cells, platelets and plasma [25]. There are several approaches to simulate blood flow considering it as a particulate system [26,27] but also as a continuum multiphase system [28,29]. The particulate system approach is successfully considered in several works, like the one from Stamou et al. comparing Newtonian and Non-Newtonian Models [30].

Another challenge is the consideration of a proper viscous model that fits with the blood system. Viscosity models for blood have been proposed in recent years. For example, there is a study based on the Casson model with parameters that are dependent on the local haematocrit [31].

The first aim of this project was to study the interaction between blood flow and the catheter inserted. A second aim of the work was to study the mixture of blood with infused fluids to evaluate the conditions of fluid dynamics of the mixture itself. This involves the precise study of the path of blood through the veins and the catheter through the venous tube itself. It was not the objective of this work to perform advances in the development of blood models.

The following hypotheses were proposed:

Hypothesis 1 (H1). *Catheter insertion significantly alters blood flow, increasing its velocity due to reduced passage.*

Hypothesis 2 (H2). *The mixture of blood with the substances infused occurs homogeneously in the venous area prior to entry into the heart.*

To carry out this study, a very basic CFD approach was considered complemented by experimental validation through Doppler measurements. In this study, we assumed the blood to be a continuum and a linear model for viscosity. A multiphase approach was used to model not the blood, but the interaction between the blood and the medicines infused through the catheter. Thus, the assumptions caused limitations on the results of this basic research, but allow for providing a description of the abovementioned interactions between blood, the catheter and the medicines infused in a large volume situation. More robust modelling might not allow for such dimensions due to the computational cost. Additionally, recent published studies still use a similar modelling approach to the one used in this work [32]. Further works should include these improvements.

2. Methodology

2.1. Software Used and Simplifications Considered

The simulations were carried out with the software Ansys® 2023 R2 (Universitat Rovira i Virgili license) [33]. Specifically, the following programs were used:

- Ansys® DesignModeler™ 2023 R2. Software used to design the models to be simulated.
- Ansys® Fluent™ Meshing 2023 R2. Software used to establish the mesh on the previously created models and solve the physics including the necessary models.
- Ansys® CFD-Post 2023 R2. Software used to analyse the results and obtain the figures shown in the report.

Assumptions: The tubular structure of blood vessels is irregular and changes according to the biological characteristics of the individual. Nevertheless, in this work, it was considered that venous geometry could be defined precisely and regularly as non-distensible cylindrical vessels that always remain in the same position [34,35]. It was also assumed that just as the studied veins converge at points from which new veins form, the increase in diameter is progressive and linear. The last assumption was that the blood velocity was defined with constant values.

2.2. Parts of the Study

The study was divided in two parts. The first part studied the influence of the catheter on blood flow and its velocity from the basilic vein to the vena cava, considering two different blood inlet velocities of 0.24 m/s and 0.15 m/s. These velocities were selected according to data from the literature [36–38], which were, afterwards, compared to results obtained from the Doppler measurements. Nevertheless, it should be noted that these values change in each individual due to several factors. The reason for selection of two values was also to perform a sensitivity analysis. For each velocity, two simulations were performed: a simulation of the blood flow without the presence of the catheter and a simulation with the presence of the device.

The second part studied the quality of the mixture of blood with fluids infused through the catheter in the final section of the route of this device. This part comprised four different simulations where different fluids and velocities were combined.

Part 1

The influence of the catheter on the blood flow from the basilic vein to the vena cava was examined, studying two different blood velocities: 0.24 m/s and 0.15 m/s with and without the presence of the catheter. The blood velocity values were selected through the results of a Doppler ultrasound provided by the Arnau de Vilanova University Hospital in Lleida and contrasted with studies and medical articles, cited in the bibliography [36–39].

- Simulation 1: average inlet velocity of blood: 0.24 m/s
  - Simulation 1.1: blood from the basilica vein to the vena cava without catheter.
  - Simulation 1.2: blood from the basilica vein to the vena cava with catheter.
- Simulation 2: average inlet velocity of blood: 0.15 m/s

- Simulation 2.1: blood from the basilica vein to the vena cava without catheter.
- Simulation 2.2: blood from the basilica vein to the vena cava with catheter.

Prior to the resolution of the first part, a length of the venous system prior to the section under study was simulated in order to be able to define an already developed fluid as flow inlet (avoiding the use of a velocity flow inlet surface with a constant value). The values of each element of the mesh were extracted from this previous simulation and were used as the input boundary conditions of the simulations. Because of the Reynolds number, the laminar viscous model was chosen, and the hemodynamic properties of the blood phase were defined, indicating a density of 1055 kg/m^3 [40,41] and a viscosity of 0.004 Pa·s [42,43]. The simulation was carried out taking gravity into consideration. Finally, the calculation was performed in iterations considering a tolerance of magnitude less than 10^{-7} in the results. In the post section, several planes were created for the analysis and to obtain the result figures. On these planes, the contours and velocity vectors were represented. Two segments were also defined in the basilica vein and the brachiocephalic venous trunk for analysis of data. Finally, the values of the average volumetric velocity and of each sectional slice were found.

Part 2

In this part, the confluence of blood with the fluids infused through the three lumens of the catheter was studied in a delimited area between the subclavian vein and the cava.

Simulations were split into two different cases. In the first case, only two lumens were considered to carry fluid. In the second case, three lumens carried fluid. This is justified by real-life situations. Moreover, the velocity of one of the fluids inserted in the catheter was considered as a variable to be able to contrast the influence of the phenomenon studied in part one.

- Simulation 1: Study with two lumens
  - Simulation 1a: fluid therapy (physiological serum) at constant velocity and inotropic agent (Noradrenaline) at 35 mL/h.
    - Proximal lumen: insertion of inotropic agent at 0.648 m/s.
    - Distal lumen: insertion of fluid therapy at 0.673 m/s.
  - Simulation 1b: fluid therapy at constant velocity and inotropic agent at 15 mL/h.
    - Proximal lumen: insertion of inotropic agent at 0.278 m/s.
    - Distal lumen: insertion of fluid therapy at 0.673 m/s.
- Simulation 2: Study with three lumens
  - Simulation 2a: Fluid therapy at constant velocity. Inotropic agent dosage of simulation 1a was repeated and TPN (total parenteral nutrition) was added in the medial lumen.
    - Proximal lumen: insertion of inotropic agent at 0.648 m/s
    - Medial lumen: insertion of TPN at 0.833 m/s.
    - Distal lumen: insertion of fluid therapy at 0.673 m/s.
  - Simulation 2b: Fluid therapy at constant velocity, inotropic agent dosage of simulation 2a was repeated and TPN was added in the medial lumen.
    - Proximal lumen: insertion of inotropic agent at 0.278 m/s.
    - Medial lumen: insertion of TPN at 0.833 m/s.
    - Distal lumen: insertion of fluid therapy at 0.673 m/s.

To verify the effect of surface tension and gravity in the simulation, three different simulation tests were carried out in part 2. There are several dimensionless numbers that describe flows such as Re, which characterizes the motion of a fluid, and We, which indicates the relevance of surface tension. When Re is greater than 1, the surface tension is irrelevant if We is greater than 1. These elements led to the assumption of non-consideration of the surface tension.

Given the Re number, a laminar flow simulation and a multiphase model with four phases were considered. For the blood phase, a velocity of 0.24 m/s was defined, and in each phase of fluid inserted through the catheter, the velocities specified above were used. In this section, the rest of the properties of fluid dynamics were also defined. The blood properties were not modified from the first part. Gravity was also considered, although it could have been neglected from test simulations performed that showed no changes in the results, as demonstrated in previous works [44]. The surface tension between phases and with the walls of the system were indicated as zero. Two planes were created to obtain transversal sections in the catheter lumens as well as two cross-sections in the vena cava and the brachiocephalic venous trunk. On these transversal planes, the volumetric fraction contour and streamlines (the path of the particles of each infused fluid) were represented. On the cross-section surfaces, the contour of the volumetric blood fraction was represented.

Finally, the quality percentage (Q) values of the mixture of each simulation were calculated using our own experimental equation (Equation (5)). This equation is based on the fraction concept considering the inlet flow rates of the blood and the medicines. This parameter provides a number between 0 and 100% to evaluate the quality of the mixture between the blood and the various fluids inserted through the catheter. A score of 100% would represent a theoretically perfect and homogeneous mix, while 0% would indicate the worst quality.

$$Q = 100\% \cdot abs\left(1 - \frac{\sum_{i=1}^{n} abs(x_{ideal} - x_i)}{\sum_{i=1}^{n} (x_{ideal}(1 - 0.99 \cdot x_i))}\right) \quad (5)$$

where x_{ideal} is the ideal blood volumetric fraction and x_i is each value of volumetric fraction in the selected surface. In this study, different values for x_i were considered for each simulation depending on the flow ratio of the inserted fluids.

Tables 1 and 2 present the calculations of the ideal blood volumetric fraction for the study of the quality of the mixture between blood and inserted fluids during the second phase of the simulation.

Table 1. Reference parameters for the study of the quality of the mixture in the case of two lumens (simulation 1).

Simulation 1a						
	Venous trunk radius (mm)	Venous trunk section (mm^2)	Blood velocity (mm/s)	Flow (mm^3/s)	Flow (mL/h)	
Blood	8.35	219.04	240	52,569	189,250	
Noradrenaline					63	
Fluid therapy					35	**Ideal blood Vol. Frac.**
				Total:	189,348	**0.99948**
Simulation 1b						
	Venous trunk radius (mm)	Venous trunk section (mm^2)	Blood velocity (mm/s)	Flow (mm^3/s)	Flow (mL/h)	
Blood	8.35	219.04	240	52,569	189,250	
Noradrenaline					63	
Fluid therapy					15	**Ideal blood Vol. Frac.**
				Total:	189,328	**0.99959**

Table 2. Reference parameters for the study of the quality of the mixture in the case of three lumens (simulation 2).

Simulation 2a						
	Venous trunk radius (mm)	Venous trunk section (mm^2)	Blood velocity (mm/s)	Flow (mm^3/s)	Flow (mL/h)	
Blood	8.35	219.04	240	52,569	189,250	
Noradrenaline					63	
Fluid therapy					35	
Parenteral nutrition					42	**Ideal blood Vol. Frac.**
				Total:	189,390	**0.99926**
Simulation 2b						
	Venous trunk radius (mm)	Venous trunk section (mm^2)	Blood velocity (mm/s)	Flow (mm^3/s)	Flow (mL/h)	
Blood	8.35	219.04	240	52,569	189,250	
Noradrenaline					63	
Fluid therapy					15	
Parenteral nutrition					42	**Ideal blood Vol. Frac.**
				Total:	189,370	**0.99937**

2.3. Simulated Model

For this study, it was necessary to focus on the venous vessels corresponding to the upper and intrathoracic limbs. The model was designed from an adoption of the anatomical model proposed by Netter [45]. The veins considered were the basilica, cephalic, subclavian, internal jugular, brachiocephalic venous trunk and superior cava. The basilica vein and the cephalic vein are the main drainage vessels of the arm. They originate on the back of the hand and run down the arm to the beginning of the shoulder, where they join to form the axillary vein. The axillary vein gives rise to the subclavian vein and it extends to the medial end of the clavicle. The jugular vein, on the other hand, originates in the jugular foramen of the skull and runs along the neck until it reaches the end of the subclavian vein, with which it joins to form the brachiocephalic venous trunk. The right and left brachiocephalic venous trunks are directed towards the centre of the thorax, where just before reaching the heart they join to form the superior vena cava [46]. Finally, the vena cava extends into the heart.

The anatomy of blood vessels undergoes significant changes in each person, influenced not only by their gender or age, but also by individual factors, including the physiological, morphological and anatomical characteristics of each individual. This variation occurs in the size of the vessels and their arrangement within the body.

Table 3 contains the measurements of the veins, obtained from bibliographic data and measurements made in this study with an ultrasound scanner (see later sections).

Table 3. Vein dimensions.

Veins	**Basilica [47,48]**	**Cephalic [49]**	**Subclavian [50,51]**	**Intern. Jugular [51–53]**	**Brachiocephalic Trunk [54]**	**Cava [54]**
Radius [mm]	2.7	1.44	3.69	6.38	8.35	11.65
Length [cm]	28	26.5	18.85	13.5	4.57	4.57

Catheter

To know the dimensions of the catheter, a standard catheter provided by the Arnau de Vilanova University Hospital in Lleida was taken as a reference. A catheter is inserted into the centre of the venous tube at an oblique angle of between 30 and 40°. It is a device composed of three equidistant cylindrical tubes (lumens). The catheter section is circular and has a diameter of 2.181 mm.

To accurately determine the area and diameter of each lumen, the catheter was dissected and a macro photograph of the diameter section of the device was obtained (Figure 1). The image was later processed with the open-source program ImageJ, version 1.54j [55].

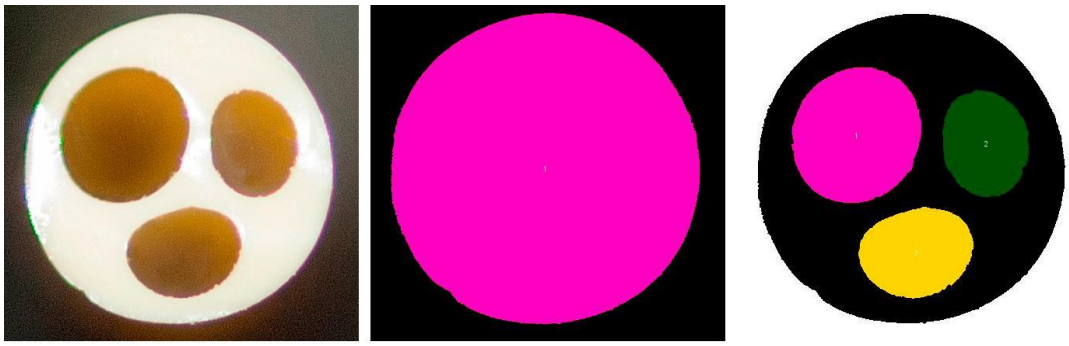

(**a**) (**b**) (**c**)

	Area (mm²)	Std. Dev. (mm²)	Perimeter (mm)	Diameter (mm)	Std. Dev. (mm)	Circularity
Lumen 1	0.687	0.026	3.156	0.935	0.010	0.867
Lumen 2	0.369	0.014	2.351	0.685	0.008	0.839
Lumen 3	0.398	0.015	2.438	0.712	0.008	0.841
Catheter	3.737	0.142	7.448	2.181	0.024	0.847

Figure 1. Sectional section of the catheter. (**a**) Photograph of the catheter section, (**b**) digitization of lumen 1, (**c**) digitization of the entire catheter.

To design the model (Figure 2), the chosen reference system designated the components x and y forming a horizontal plane and z being the vertical component. The coordinate origin was located at the beginning of the basilic vein, in the centre of the circumference. Initially, the axis lines of the venous system were drawn and then the sweep tool was applied. The basilic vein started from the horizontal plane and extended in the horizontal component. In the case of the cephalic vein, the plane was turned over to achieve oblique growth. The subclavian vein was traced on a semi-circumference that started from the elevated cephalic plane, displaced in the y and z components. The jugular vein, the brachiocephalic venous trunk and the vena cava started from the slightly turned horizontal plane. Finally, the right brachiocephalic venous trunk was traced from a circumference (which was kept at 90°) that started from the left brachiocephalic venous trunk, tangent to the semi-circumference of the subclavian vein. Subsequently, a straight section was added to define the initial section of the right brachiocephalic venous trunk. Considering the sizes of each vein, the circumference of each blood vessel was traced, and then expanded to obtain three-dimensional vessels. The small veins were expanded where they entered the larger ones. In the junctions of the subclavian vein with the cephalic and basilic veins, a junction with a conical structure was designed to simulate the progressive increase in the diameter of the vessels. This procedure was reproduced at the junction between the brachiocephalic venous trunk and the vena cava to simulate the progressive growth of the latter vein.

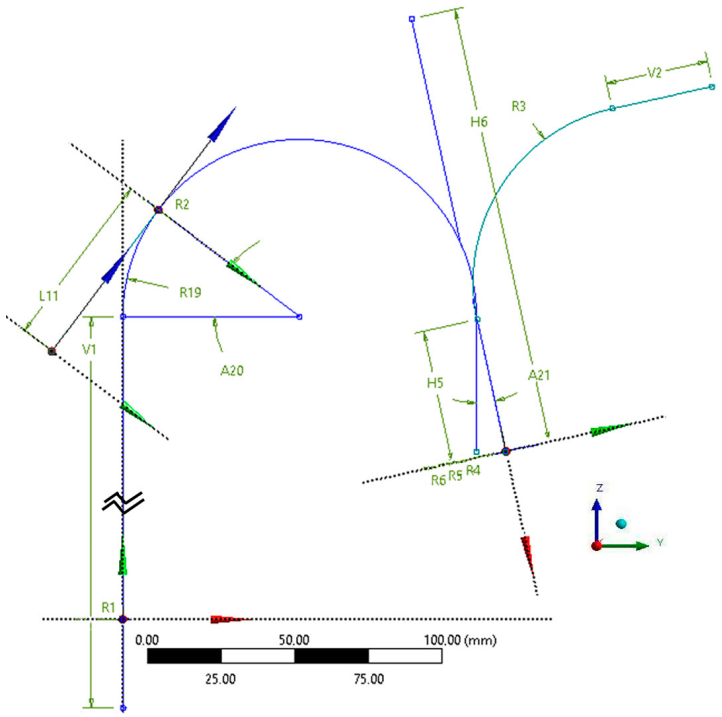

Dimension	R1	R2	R3	R4	R5	R6	R19
Size	2.7 mm	3.69 mm	60 mm	6.38 mm	8.35 mm	11.65 mm	60 mm
Dimension	A20	A21	H5	H6	L11	V1	V2
Size	37°	12.2°	45.7 mm	150 mm	60 mm	170 mm	35 mm

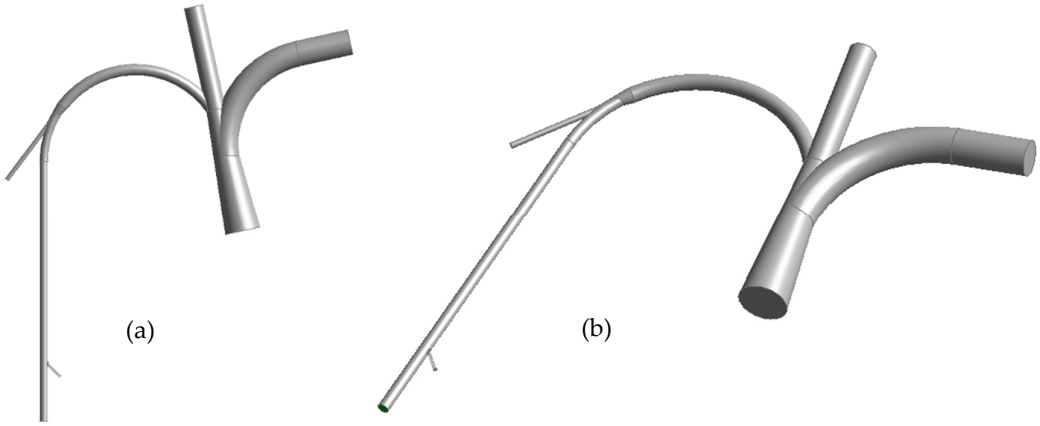

Figure 2. Venous geometric model. (**a**) Model without catheter, (**b**) model with catheter.

Subsequently, the catheter was designed. The measurements are specified in the following section. The catheter starts from a horizontal plane turned 35° relative to the vertical component z, slightly displaced in component y, so that the first section is located outside the blood vessel. As it enters the basilic vein, it curves until it is parallel to the walls of the basilic vein. The device travels through the venous system from this point, following the path of the veins, always being in the centre of the circumference of the vessels. The catheter extends until reaching the middle of the brachiocephalic venous trunk. Inside, there are three ducts that correspond to the 3 lumens.

This geometric model was used in the first part of the simulation. In the second part, it was only necessary to study the last section of the system and therefore, the system was simplified, maintaining the vena cava, the left brachiocephalic venous trunk, the jugular venous vein and a small part of the subclavian vein and the right brachiocephalic venous trunk. With respect to the catheter, the holes of the three lumens were added.

Mesh quality

The geometric structure of the blood system was defined through a mesh, which involved interconnected finite elements (Figure 3).

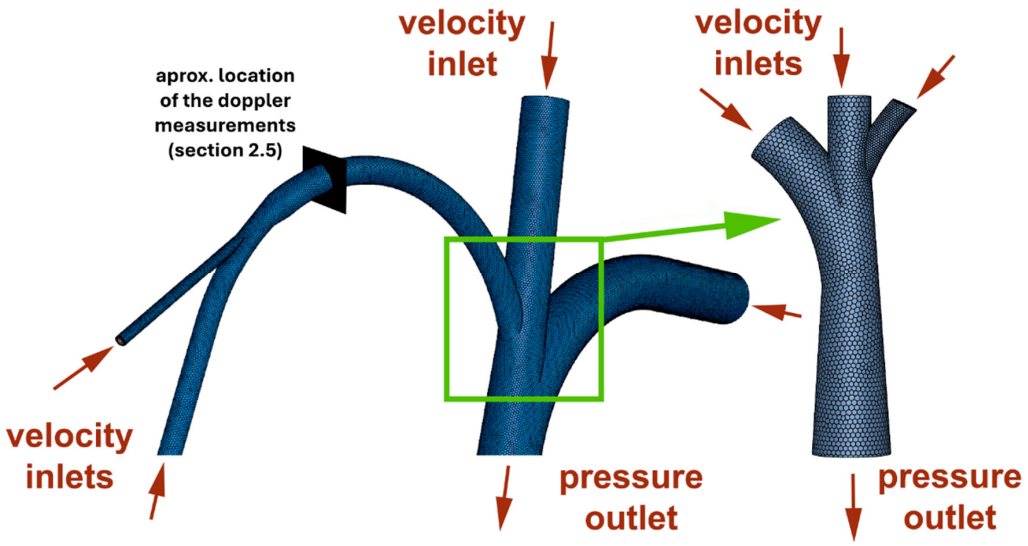

Figure 3. Phase 2 geometric model mesh view.

The quantity of these elements has significant effects on the accuracy of the simulation results and, consequently, it is essential to evaluate the quality of this mesh to ensure optimal results. Quality parameters were analysed to ensure their independence from the results (Table 4).

Table 4. Mesh evaluation results.

Simulation		Part 1 Pre-Catheter	Part 1 Post-Catheter	Part 2
Skewness	Minimum	8.331×10^{-5}	9.334×10^{-5}	1.939
	Maximum	0.7952	0.9242	0.8486
	Average	0.01830	0.02539	0.03266
Aspect ratio	Minimum	1.374	1.375	1.372
	Maximum	32.18	69.50	43.39
	Average	4.828	4.511	3.807
Number of cells		376,516	447,340	365,190

In the evaluation carried out in the system under study, three aspects were considered:

- The number of cells, which specifies the number of elements that make up the mesh.
- Asymmetry or skewness, which is the angular measure of the quality of the element with respect to the angles of the ideal types of elements. The acceptable range of skewness is from 0 to 0.5 [56]. The values obtained, therefore, were acceptable.
- The aspect ratio is defined as the ratio between the shortest length of the element and the longest length of the element. An aspect ratio of 1 is a perfectly shaped tetrahedral element [57]. The values obtained were acceptable.

The result of this evaluation confirmed that the mesh used was of sufficient quality.

2.4. Drugs

To know the properties of the drugs administered and to make the appropriate calculations, the technical data sheets of each drug provided by the Pharmacy Service of the Arnau de Vilanova University Hospital in Lleida were consulted. To carry out the project,

documents with the properties of the fluids to be studied were obtained. The information was contrasted with a medical study article that provided some viscosity data. In the case of inotropic drugs (Noradrenaline), the dose administered varies depending on the patient's hemodynamic situation. In the calculations, the mass of the patient was taken as 60 kg and therefore, the average range selected was from 0 to 40 mL/h. The values of 15 and 35 mL/h were chosen to carry out the experimental simulations. Considering the following cross sections of the lumens, Tables 5 and 6 show the calculations performed on the fluid dynamics data of the simulated fluids during the second part of the simulation.

Table 5. Properties of fluids infused in the study with two lumens.

	Flow Rate (mL/h)	**Flow Rate m^3/s**	**Velocity m/s**	**Density (kg/m^3)**	**Viscosity (kg·s/m)**
Physiological serum (lumen 1, distal)	63	1.75×10^{-8}	0.673	1004–1006	2.5×10^{-3}
Inotropic drug 2 (lumen 3, proximal)	35	1×10^{-7}	0.648	997 (water)	1.05×10^{-3}

Table 6. Properties of fluids infused in the study with three lumens.

	Flow Rate mL/h	**Flow Rate m^3/s**	**Velocity m/s**	**Density (g/L)**	**Viscosity (kg·s/m)**
Physiological serum (lumen 1, distal)	63	1.75×10^{-8}	0.673	1004–1006	2.5×10^{-3}
PTN (lumen 2, medial)	42	1.167×10^{-8}	0.833	1065	1.05×10^{-3}
Inotropic drug 1 (lumen 3, proximal)	15	4.17×10^{-9}	0.278	1000 (water)	1.05×10^{-3}

- Cross section of lumen 1 (distal): 2.6×10^{-2} mm^2
- Cross section of lumen 2 (medial): 1.4×10^{-2} mm^2
- Cross section of lumen 3 (proximal): 1.5×10^{-2} mm^2

2.5. Doppler Ultrasound

To acquire information about blood velocity (complementary to the data obtained bibliographically) and to validate the results obtained in the simulations, Doppler ultrasound measurements were performed in the basilic and subclavian veins.

This technique allows us to know the speed and direction of blood flow. When ultrasound is emitted into the bloodstream, erythrocytes act as reflecting elements and through the Doppler equation their velocity can be calculated (Equation (6)).

$$V = \frac{(F_E - F_R) \cdot K}{2 \cdot F_E \cdot \cos \alpha} \quad (6)$$

where V (m/s) is the velocity of red blood cells at a given instant, F_E (Hz) is the emission frequency, F_R (Hz) is the reception frequency, K is the speed of sound in blood (1540 m/s) and α is the angle formed by the sound beam and the direction of flow.

The measurements were carried out at the Arnau de Vilanova University Hospital in Lleida during the summer of 2023 with a MyLab^{TM} Gamma ultrasound machine (Esaote, Genova, Italy; by trained intensive care staff). Pre- and post-catheter insertion measurements were performed. Figure 3 shows the approximate location of the measurements area. Parameters used in the equipment are indicated in Table 7.

Table 7. Parameters used in the Esaote MyLab^{TM} Gamma ultrasound machine.

Imaging Parameters			
Depth			44 mm
Dynamic range/Dynamic compression/Density/Gray map			8/3/1/1
Sample volume size and depth			2/16 mm
Imaging gain			-
X-View Algorithm or CrystaLine Imaging/M-View algorithm			C3/1
Persistence			1
Doppler angle correction			60°
Colour Flow Parameters		**Doppler Parameters**	
Colour frequency	5.0 MHz	Doppler frequency	5.0 MHz
Pulse repetition frequency	1.9 kHz	Pulse repetition frequency	6.1 kHz
Smooth/Density	M/1	Dynamic range	7/4
Colour gain	-	Doppler gain	50%
Wall filter	3	Wall filter	100 Hz
Persistence	3		

3. Results and Discussion

3.1. Study of the Interaction Between the Catheter and the Blood Flow

3.1.1. Analysis with Blood Velocity: 0.24 m/s

Figure 4 presents the velocity contour of the systems at a general level in cross-section. In a developed fluid, the velocity profile was parabolic which is typical in these contexts (Poiseuille flow). The flow reached its maximum velocity in the centre of the duct and decreased to zero at the walls. This phenomenon was observed in the simulation without the presence of a catheter (Figure 4a), where the maximum velocity of the blood was in the axis of the vein and as it approached the walls of the veins, it decreased until it cancelled out. At some points in the system, where the veins converge, fluid-tight areas of very low speeds were noticed, produced by the direction of the fluid before it joins the vein. With the presence of the catheter (Figure 4b), two separate spaces were observed because of the representation of the venous device in 2D. But in 3D, there was only one cavity. In this system, a slight modification was observed in the distribution of fluid near the catheter walls and, although similar fluid-tight areas were observed in both systems, in the presence of the catheter, there were some fluid-tight spots that were not observed in the catheter-free simulation. Maximum blood velocities were about 1.5% higher in the case of the presence of the catheter. This was an expected result since the catheter reduced the cross-sectional area of the vein where blood flows, and the velocity depends on this.

Analysing the velocity vectors, in the simulation without catheter, a regular flow distribution with a single parabolic profile was obtained. On the other hand, in the system with catheter, the fluid distribution varied slightly: there were two parabolic profiles due to the presence of the catheter acting as a wall. Likewise, a slight increase in speed was observed since the presence of the catheter reduced the area of circulation of the fluid. The fact that the profile conformed very closely in both cases to a parabola and did not have a flat top, corroborated its laminar behaviour. This is clearly visualized in Figure 5. In the case with catheter, the flow described two parabolic velocity profiles with no notable differences between them, separated by the catheter representing a central wall. The blood reached its maximum speed at the most separated points of the walls of the veins and the catheter. In absence of catheter, the blood was distributed in a single parabolic profile and reached its maximum velocity at the central point of the vein, the most distal to the walls.

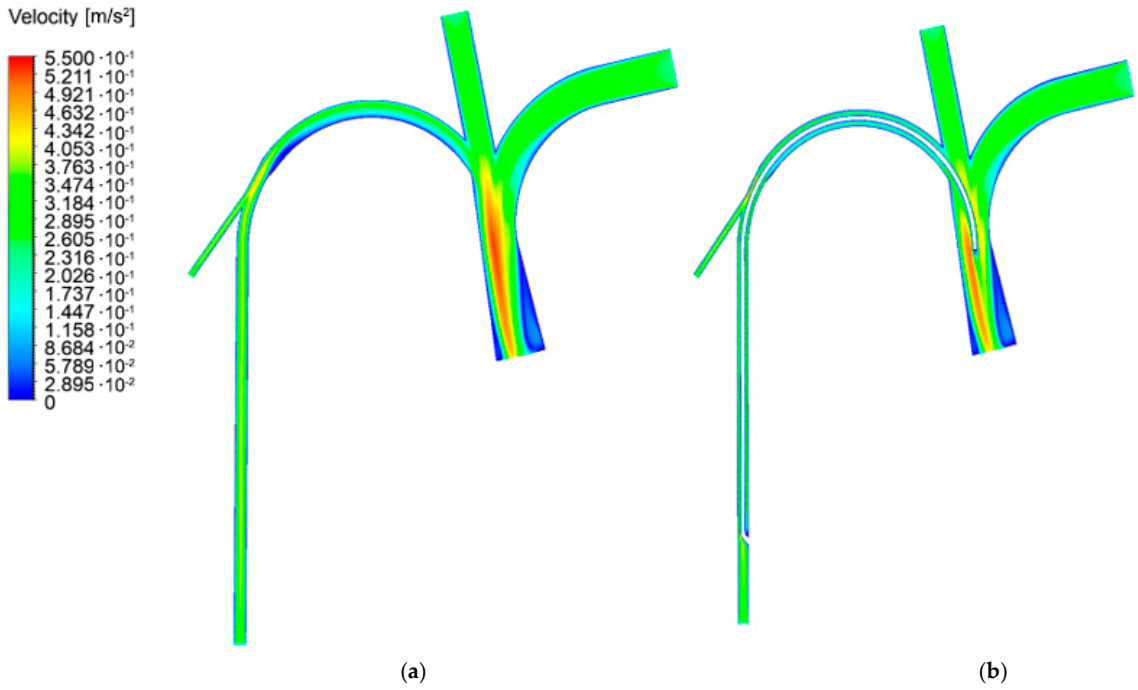

Figure 4. Speed contours in the central cross-section. (**a**) Pre-catheter system, (**b**) post-catheter system.

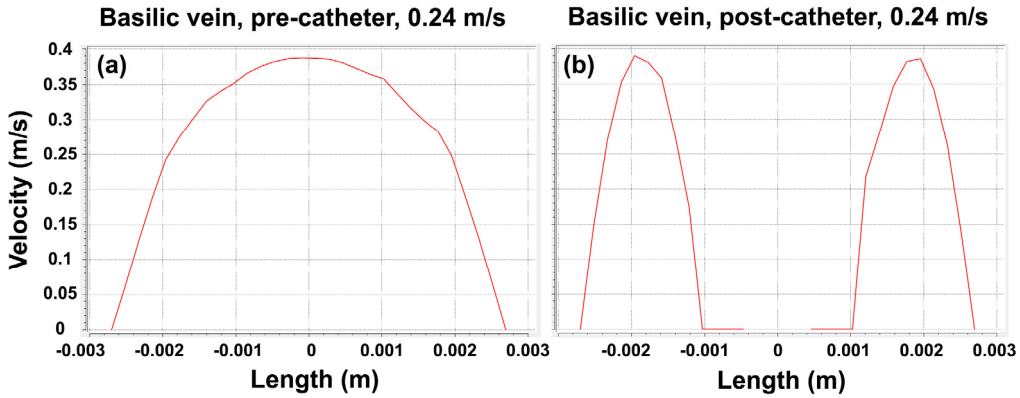

Figure 5. Velocity profiles in a central section of the basilic vein. (**a**) Pre-catheter system, (**b**) post-catheter system.

In the system without catheter, in the lower part of the subclavian vein, a fluid-tight area was generated where the velocity was greatly reduced due to the direction of the fluid flow before entering the curvature. The blood that came out of the basilic vein had a very vertical direction which, when it entered the curvature, caused the blood to impact the upper wall of the vein. The fluid that came from the cephalic vein had less flow, which caused it to be incorporated into the fluid of the basilic vein and take its direction. On the other hand, in the system with catheter, there was a considerable reduction in the fluid-tight area that occurred in the first system, homogenizing the velocity of the fluid.

Figure 6 presents a sectional cut in the subclavian vein that allowed observation of the phenomenon recently indicated in both simulations. The change in blood direction due to the curvature of the vein caused the velocity distribution to lose its regularity. The blood flow tried to maintain its direction perpendicular to the upper wall of the subclavian vein and a fluid-tight area was produced in the lower wall. In the catheter-free simulation, the absence of the device reduced the intensity of this phenomenon.

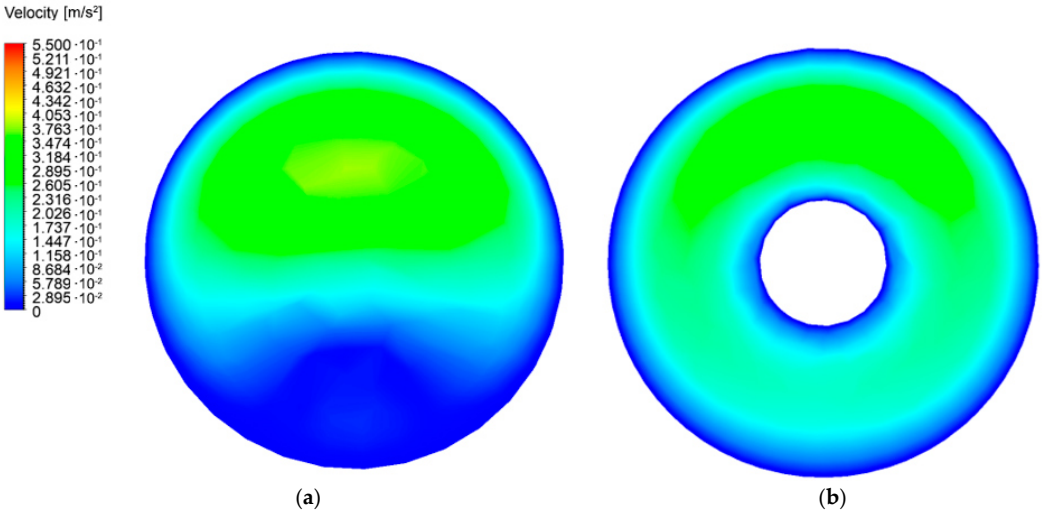

Figure 6. Velocity contours in a sectional cut of the subclavian vein. (**a**) Pre-catheter system, (**b**) post-catheter system.

As for the brachiocephalic venous trunk, there was an irregular distribution of velocities caused by the confluence of blood from the jugular vein and the subclavian vein, although it presented certain symmetries. In the simulation with catheter, certain areas of higher velocity were observed. This was caused by the decrease in the passage area due to the insertion of the catheter into the venous duct, which caused the blood flow speed to increase to maintain constant flow.

The results in the final section of the vena cava in sectional cut did not show relevant differences in the cases with and without a catheter at the end of the cava, neither in distribution nor velocity of the fluid. Only small changes were observed in the distribution of areas where the velocity was low. In the flow of the fluid through the vein, there were points where the velocity of the particles decreased, changed their direction, and vorticities were created, as shown by the velocity vectors. This happened in both the pre- and post-catheter cases. However, defining whether a flow was laminar or turbulent depended on Reynolds number and not on the vortices present in the fluid. There can be vorticities in a laminar fluid, as it is only considered turbulent when the chaotic flow is in a transient state. As for the distribution of fluid through the veins, it did not change considerably depending on the presence of the catheter (Figure 7b), nor did the velocity at the heart inlet.

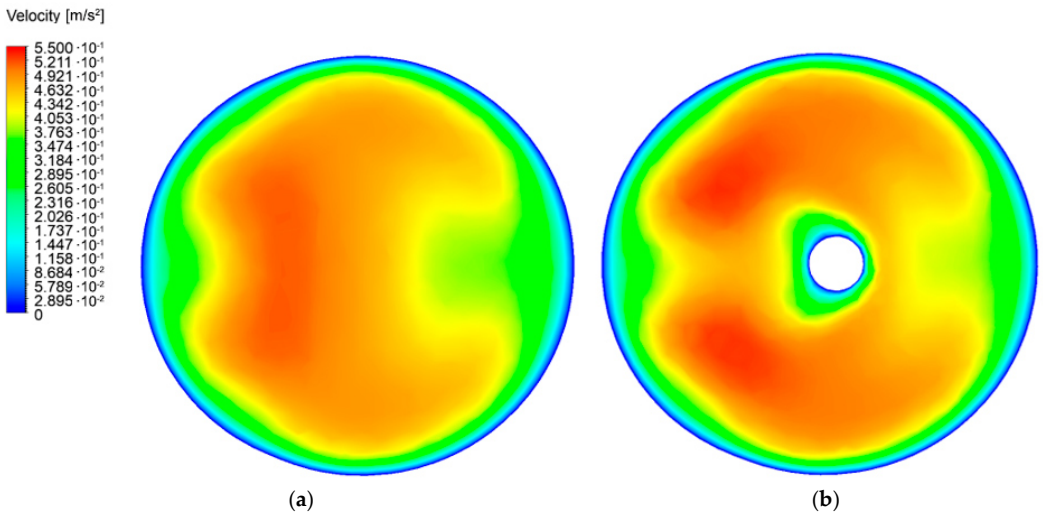

Figure 7. Velocity contours in a sectional cut of the brachiocephalic venous trunk. (**a**) Pre-catheter system, (**b**) post-catheter system.

Analysing the velocity contours in a cross-section plane, fluid distributions were quite similar in the simulation of the vein with catheter compared to without. In both cases, there was a fluid-tight area on each side and a higher speed profile concentrated on one side. The fluid flowed through the vena cava and following the trajectory provided by the final location of the catheter.

Table 8 presents the average velocity values in the study volume and various sectional sections. The general average velocity, at volumetric level and around the transverse plane, took very similar values and did not present a notable variation in the post- and pre-catheter comparison. A notable tendency of the average velocity to be higher in the diameter cuts in the post-catheter simulation could be observed. It was caused by a reduction in the passage of fluid in the presence of this device in the veins.

Table 8. Average velocity values in several zones, 0.24 m/s inlet velocity case study.

Pre-Catheter	Post-Catheter
Average blood velocity across the study volume	
0.2624 m/s	0.2674 m/s
Average velocity in the section of the basilic vein	
0.2371 m/s	0.2810 m/s
Average velocity in the section of the subclavian vein	
0.2991 m/s	0.3113 m/s
Average velocity in the section of the brachiocephalic venous trunk	
0.3860 m/s	0.3983 m/s
Average velocity in the section of the vena cava	
0.2673 m/s	0.2708 m/s

In general, we detected a slight increase in the average velocity as the diameter of the veins through which the blood flows increased. But in the vena cava, the last vein of the simulated path, the average velocity was reduced again to the velocity that was found in the first vein of the path: the basilica. This difference in velocity was very relevant in veins of small diameter and became less significant as the diameter of the veins increased. This is explained by the fact that the catheter reduced a greater proportion of the cross-sectional area in veins with a smaller diameter. Although the vein entry velocity was 0.24 m/s, the average of the system in the simulation was slightly higher.

In the pre-catheter simulation, the section in the basilic vein showed a 9.6% reduction in average velocity compared to the average velocity of the general volume. In contrast, in the post-catheter simulation, the average velocity of the section in the basilic vein increased by 5.1% compared to the average volumetric velocity. Considering the average velocity of the section in the brachiocephalic trunk, this value showed an increase of 47.10% compared to the average volumetric velocity in the case of the pre-catheter simulation and 48.95% in the post-catheter simulation.

3.1.2. Comparative Analysis Between Blood Velocity 0.24 and 0.15 (m/s)

Figure 8 represents the velocity contour of a cross-section located around the union between the basilica and cephalic veins that form the subclavian vein. The distribution of blood in the two figures was very similar. In both, an almost fluid-tight area could be observed in the venous curve in which the velocity is low, close to zero. This area with low velocities was caused by the direction of the velocity of the blood before entering the corresponding vein. It should be noted that the low-speed zone in Figure 9a had a smaller fluid-tight area than in Figure 8b but, on the other hand, it gave velocity values closer to 0.

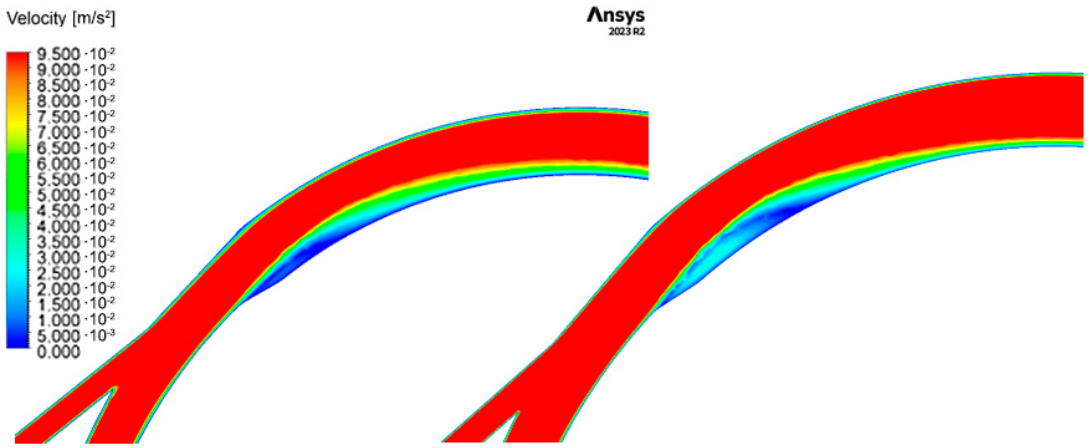

(**a**) (**b**)

Figure 8. Velocity contours of a cross-section between the basilica and cephalic veins that runs into the subclavian vein. (**a**) Blood velocity of 0.15 m/s, (**b**) blood velocity of 0.24 m/s.

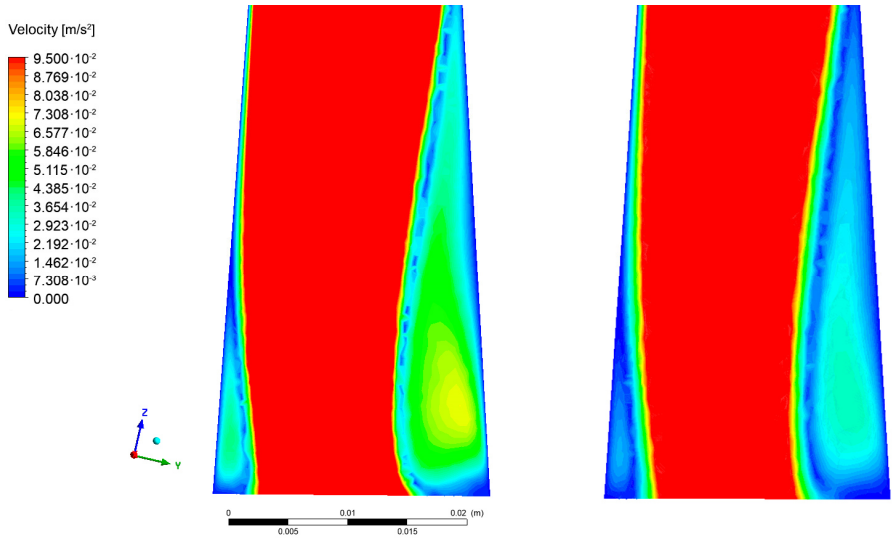

(**a**) (**b**)

Figure 9. Velocity contours of the final section of the vena cava. (**a**) Blood velocity of 0.15 m/s, (**b**) blood velocity of 0.24 m/s.

Observing the velocity vectors in the initial section of the subclavian vein, the highest velocity was in the centre of the upper region of the blood vessel, while in the lower part, a fluid-tight area with vorticities was observed. In the simulation with the highest velocity, this vortex was much more obvious, while in the simulation with the lowest velocity, the vortex was very small and only occurred at the extreme left of the low-velocity zone.

In the final section of the vena cava, an area of very low velocities was observed with some fluid-tight regions on the left and right side of the blood vessel, the latter being considerably larger. This area was slightly accentuated in the lower-speed simulation. The central velocity of this region was higher in the higher-velocity simulation while in the lower-velocity simulation, the central area of this region showed a slower velocity, resulting in the overall velocity being more homogeneous.

The comparison of the two cases with the presence of a catheter showed that the differences were almost non-existent. The consequences of this on the flow explained the effect of the different velocities. In the area of the vena cava (Figure 9), where the volume of blood per unit of time was the greatest, some slight difference was observed. In both simulations, a very low-velocity zone was highlighted including certain fluid-tight regions,

both in the left and right zones. Nevertheless, it was in the latter that a considerably extensive region was formed. These zones were formed by a central zone of reduced velocity, surrounded by an elliptical crown where the velocity was almost zero, which was accentuated in greater force in Figure 9a. The central zone exhibited higher velocities in the simulation of Figure 9b, while the velocity in this area of the simulation of Figure 9a was much more homogeneous and reduced.

Figure 10 shows a cross-section in general view of the contour of the Reynolds number. The distribution in both figures was similar. However, from the outset, it could be observed how in Figure 10a the contour represented resulted in lower values than in Figure 10b. This was because the blood inlet velocity into the first case was lower than the velocity of the second. The Reynolds number reached considerably higher values between the brachiocephalic trunk and the vena cava. This region corresponded to the area of union of the different simulated blood vessels and in which the blood velocity was higher, facts that explained the increase in the Reynolds number.

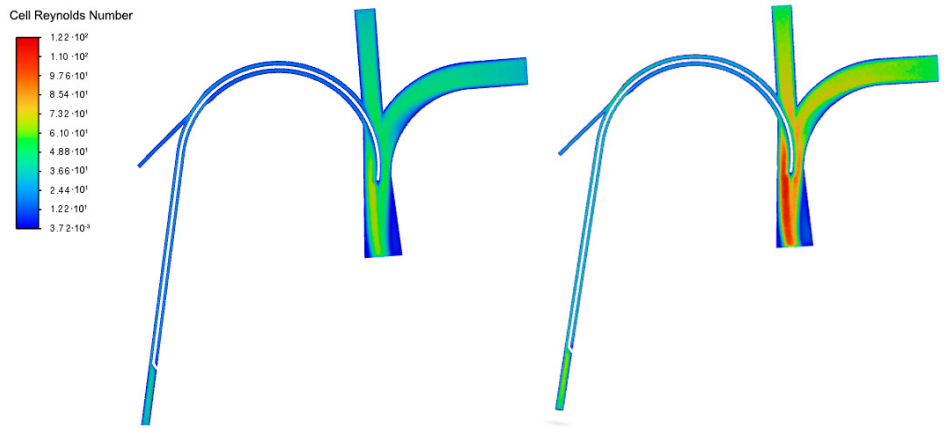

(**a**) (**b**)

Figure 10. Reynolds number contour. (**a**) Blood velocity of 0.15 m/s, (**b**) blood velocity of 0.24 m/s.

Table 9 presents the average velocity values in the study volume and various sectional sections, which can be compared with Table 8. Results are proportional to those obtained with an inlet velocity of 0.24 m/s.

Table 9. Average velocity values in several zones, 0.15 m/s inlet velocity case study.

Pre-Catheter	Post-Catheter
Average blood velocity across the study volume	
0.1637 [m/s]	0.1669 [m/s]
Average velocity in the section of the basilic vein	
0.1482 [m/s]	0.1756 [m/s]
Average velocity in the section of the subclavian vein	
0.1887 [m/s]	0.1930 [m/s]
Average velocity in the section of the brachiocephalic venous trunk	
0.2412 [m/s]	0.2489 [m/s]
Average velocity in the section of the vena cava	
0.1659 [m/s]	0.1680 [m/s]

Correspondence between simulation results and Doppler measures

Figure 11 shows the Doppler ultrasound study in the basilica and the subclavian veins before and after catheter insertion.

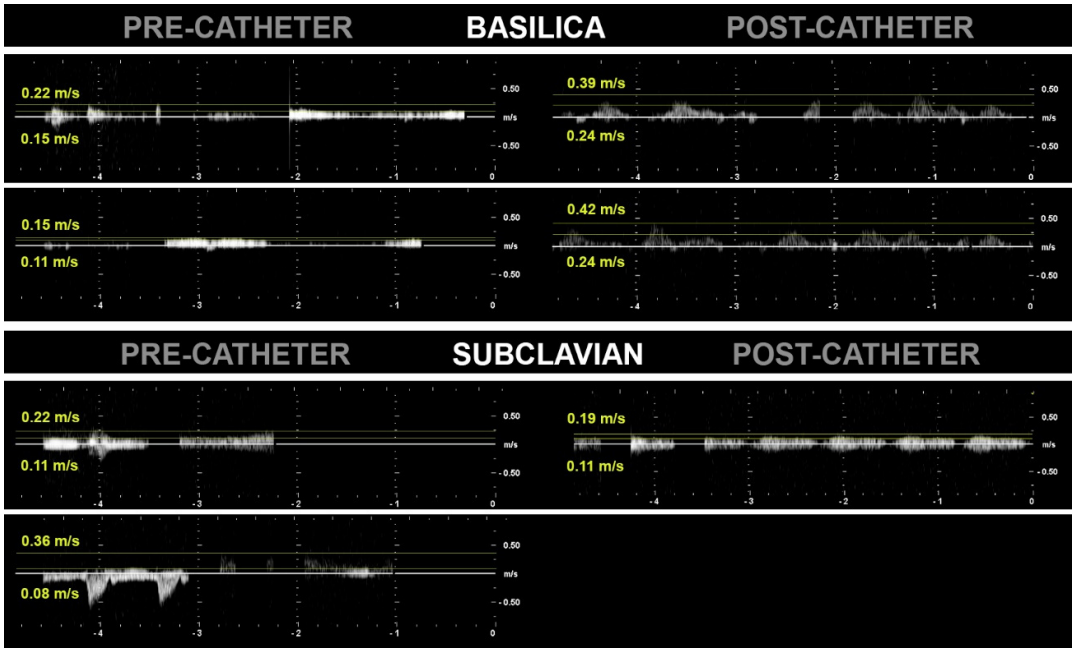

Figure 11. Doppler ultrasound results.

Results from the basilica vein were used to validate the velocity inlet boundary conditions (obtained from the literature). Doppler results showed a range of values. The highest values (0.22–0.15 m/s) agreed well with those from the literature (0.24 m/s). However, because the lowest value (0.15–0.11 m/s) was considerably different, simulations with 0.15 m/s were also performed.

Results from the subclavian vein were used to validate the simulation results. At the same position as the Doppler measurements were performed, a sectional plane was created in the simulator and the area-average velocity magnitude was computed.

For the 0.15 m/s velocity-inlet case, Doppler results for the pre-catheter subclavian vein were 0.11–0.08 m/s, while the CFD result was 0.1096 m/s. Doppler results for the post-catheter subclavian vein were 0.11 m/s, while the CFD result was 0.1010 m/s. These results show a good correspondence between the two methods, especially regarding the difference between the inlet velocity and the velocity at the subclavian vein.

3.2. Study of the Mixture Between Blood and Inserted Fluids

3.2.1. Study with Two Lumens

Figure 12 represents the volumetric fraction of fluid therapy in a cross-section in the brachiocephalic venous trunk in the distal lumen of the catheter. In the two cases represented in the figure, the velocity of the drug was identical, so there were no variations in the volumetric fraction or in the distribution of the fluid. It could also be observed that the change in velocity of the substance inserted by the proximal lumen had no effect on the flow of fluid therapy.

The volumetric fraction contour of the inotropic drug in a cross-section of the brachiocephalic venous trunk at the exit of the proximal lumen of the catheter indicated that the drug exited with the direction of the distal lumen, slightly inclined with respect to the flow of blood, but quickly joined the blood flow and took on its direction. The mixture occurred in the region of the blood vessel inferior to the catheter, since the blood and the drug move in this direction, heading to the vena cava. This increase in velocity implied the infusion of

a greater volume of this substance, which was verified since the volumetric fraction was reduced less quickly when mixed with the blood in Figure 12a.

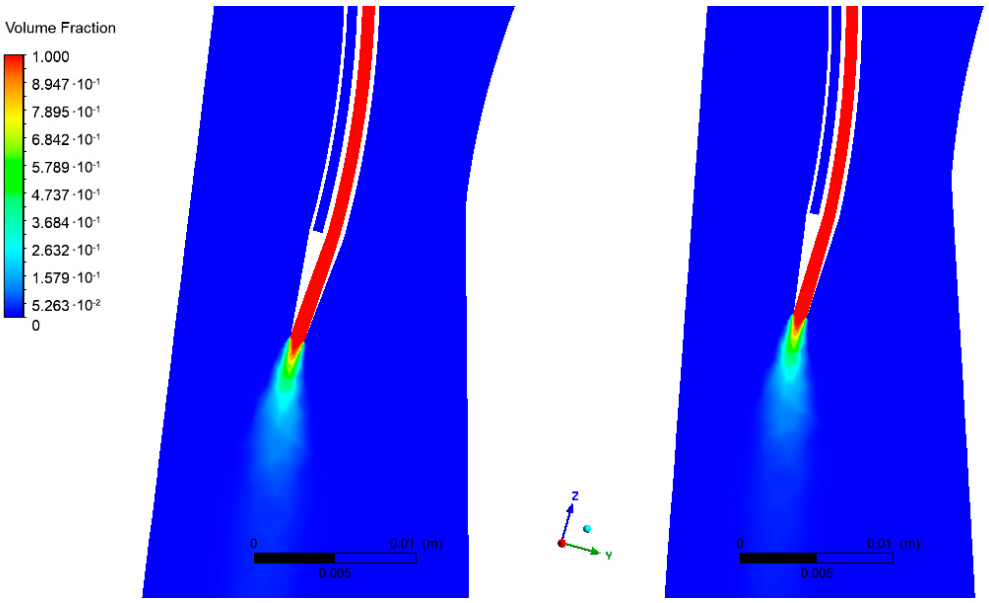

(**a**) (**b**)

Figure 12. Volume fraction contours of fluid therapy in a cross-section of the brachiocephalic venous trunk in the distal lumen of the catheter. (**a**) Inotropic drug flow rate of 35 mL/h, (**b**) inotropic drug flow rate of 15 mL/h.

Figure 13 shows the volumetric fraction of the blood in the diametrical section of the brachiocephalic trunk with a catheter in the central position. The distribution of blood through the venous tube was quite homogeneous since it occupied a large part of the diametrical surface represented in the two simulations. However, there was an area at one side of irregular distribution with a low amount of blood, and this was in a similar position in the two simulations.

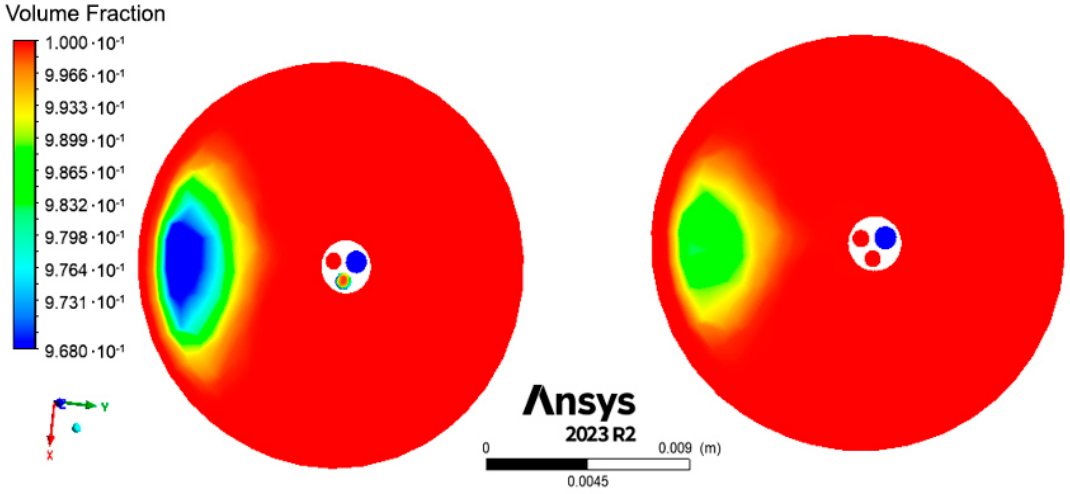

(**a**) (**b**)

Figure 13. Volumetric fraction contours of the blood in the diametrical section of the brachiocephalic trunk with a catheter in a central position. (**a**) Inotropic drug flow rate of 35 mL/h, (**b**) inotropic drug flow rate of 15 mL/h.

Figure 13a presents this region with a greater extension and a lower blood volume fraction compared to Figure 13b. The cause was that in the first simulation, the drug velocity of the proximal lumen took a higher velocity, which translated into the infusion of a greater volume of inotropic drug. It was also observed that in both simulations, two lumens of the catheter were represented with a high volumetric fraction of blood.

On the other hand, the lumen that did not contain blood inside corresponded to the fluid therapy that circulated through the distal lumen and flowed to the end of the catheter. This lumen did not have an area below the outlet of the fluid and therefore, if the sectional cut was made at whatever height, the phenomenon observed in the other lumens would never be observed. For this reason, the presence of medication and not blood could be observed in the figure. Finally, the lumen in Figure 13a, which showed an irregular volumetric fraction, corresponded to the proximal lumen. The area of this lumen in which the stagnant blood remained, also contained a small dose of inotropic drug that did not emerge into the venous environment but continued inside in the direction of the catheter. The sectional cut represented in this figure was in this transition zone between stagnant blood and residual inotropic drug that did not exit into the vena cava. Thus, the volumetric fraction of blood could not be one because it would also contain inotropic drugs (in smaller quantities).

Figure 14 represents the path of the fluid therapy particles from the distal lumen of the catheter, where this substance was inserted, in a cross-section in the lower region of the vena cava.

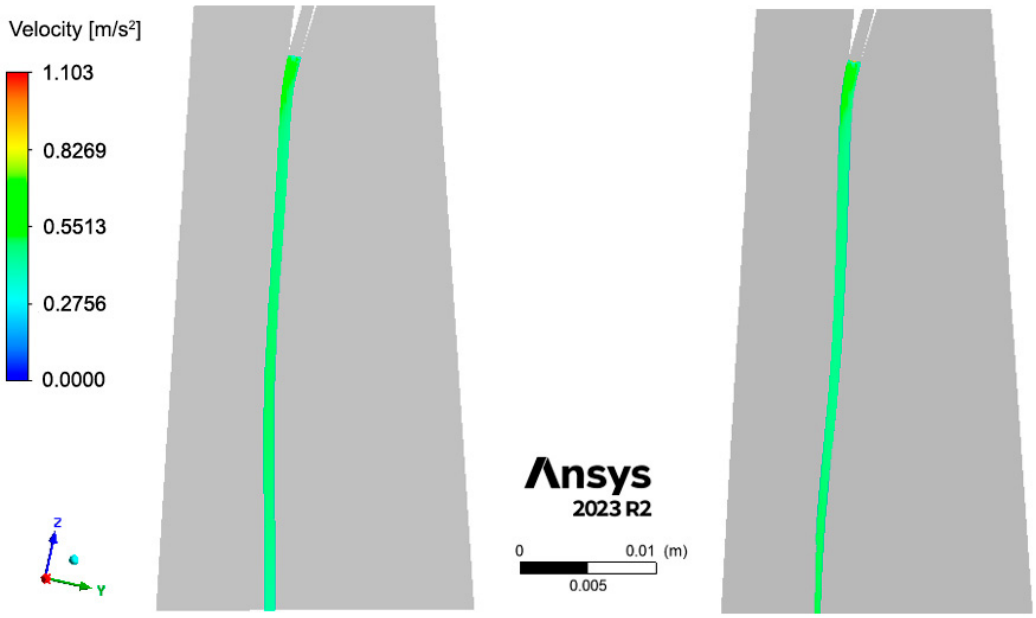

Figure 14. Path of the fluid therapy particles from the distal lumen. (**a**) Inotropic drug flow rate of 35 mL/h, (**b**) inotropic drug flow rate of 15 mL/h.

The drug emerged slightly inclined with respect to the flow of blood in the vena cava due to the arrangement of the catheter, but it did not take long to join the blood flow and follow its direction. It should be noted that the streamlines represented are conditioned by the surrounding blood which runs through the vein at a significant velocity and which influences the expansion of the drug along the sides of the venous tube. Although in both figures, the speed of the drug was maintained, slight variations could be observed in the path of the substance, influenced by the changes in speed in the inotropic drug that flowed through the proximal lumen. In the first figure, it can be seen how the trajectory described by the fluid therapy particles was almost parallel to the wall of the venous tube. It described a straighter path than in the second simulation. This was due to the influence

of the inotropic drug on the venous medium when it exited the proximal lumen at a higher velocity than in the second simulation. In Figure 14b, on the other hand, the particles of the drug described a more irregular trajectory. The cause of the observed phenomenon lay in the influence on the trajectory of the physical properties of the medium in which it was found, as well as the velocity that the inotropic drug had when it left the venous medium.

Analysing the results of trajectories of particles of the inotropic drug, it was observed that the drug flowed through the vena cava describing a trajectory almost parallel to the wall of the venous tube in both cases. Due to the high flow, it was observed that the particles of the fluid converged at the end of their path, having reached a higher velocity. This occurred precisely because of the initial insertion of the inotropic drug at a higher rate. As a result of the increase in velocity, there was also an increase in the volume of inotropic drugs.

3.2.2. Study with Three Lumens

These simulations considered the study of the third lumen: the medial lumen. Figure 15 represents the output of parenteral nutrition through this lumen. In both cases, nutrition flowed at the same velocity. Notable changes were not observed in the volumetric fraction of the fluid. However, the fluid that came out of the lumen above the medial, i.e., the proximal, went faster. This fact might influence the nutrition that spills into the environment minimally. In both simulations, nutrition emerged along the direction of the medial lumen and adopted a direction parallel to the blood flow.

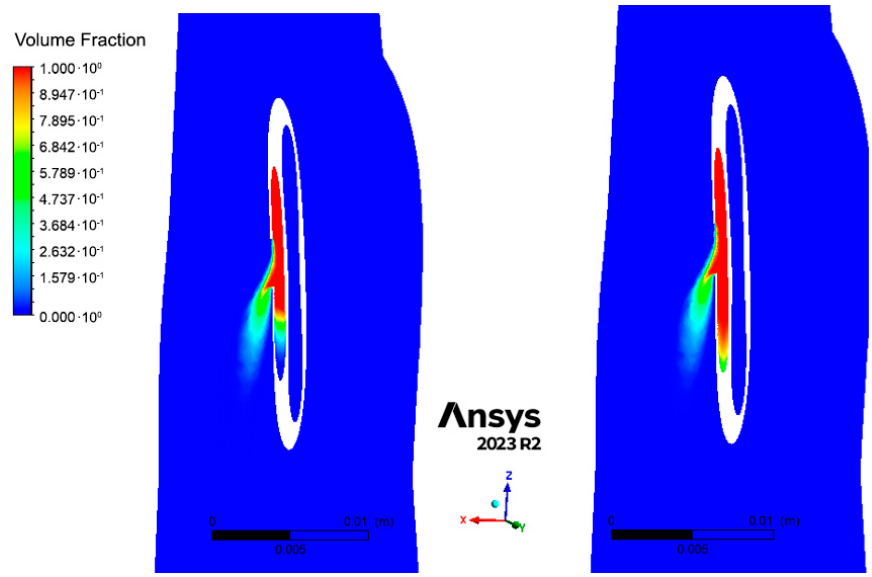

Figure 15. Contours of volumetric fraction of parenteral nutrition at the end of its lumen. (**a**) Inotropic drug flow rate of 35 mL/h, (**b**) inotropic drug flow rate of 15 mL/h.

Figure 16 represents the volumetric fraction contour of the inotropic drug in a cross-section of the venous confluence of the subclavian and brachiocephalic trunks. The outlet of the fluid through the lumen proximal to the venous medium was observed. In both simulations, the inotropic drug also exited the catheter with the final direction of the proximal lumen, adopting a direction parallel to the flow of blood.

Figure 16a shows how the fluid flowed at a higher velocity compared to Figure 16b. This occurred because the initial velocity supplied in the first figure was higher than the second. This increase in velocity implied the insertion of a greater volume of inotropic drug. This fact was corroborated by the observation of the volumetric fraction represented, since it was reduced more rapidly in Figure 16b. In both cases, in the inner zone of lumen 3 and lower than the output, an area with a very low volumetric fraction of the inotropic drug

was observed. This inner area of the device would be full of stagnant blood that would enter the catheter during the process of inserting it and purging. This finding, despite its obviosity, may be important because the blood is a biologically active fluid. Having a volume of it for some days in a stagnant but open lumen may have consequences.

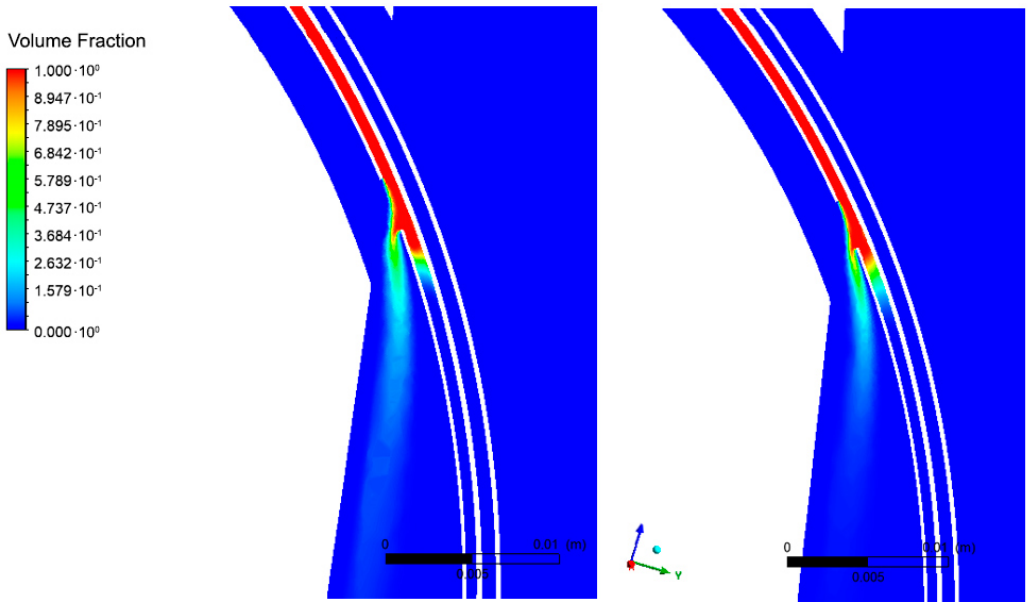

(**a**) (**b**)

Figure 16. Volumetric fraction contours of the inotropic drug in a cross-section of the venous confluence of the subclavian and brachiocephalic trunks. (**a**) Inotropic drug flow rate of 35 mL/h, (**b**) inotropic drug flow rate of 15 mL/h.

Figure 17 shows a diametrical section of the brachiocephalic trunk through a contour representation of the volumetric fraction of the blood. The blood was distributed through the vein in an analogous way in both simulations. The presence of the catheter in the centre of the venous tube was observed, as well as two areas of irregular distribution with a small amount of blood in a lateral position in both figures. These areas corresponded to the regions of confluence of fluids that shed from proximal and medial lumens, respectively. On the one hand, the irregular area closest to the catheter would be the inotropic drug that sheds from lumen 3. It corresponds to an area with a low volumetric fraction of blood since it was occupied by the inotropic drug that converged on the outside environment from the proximal lumen. The area with the least blood was the central one since it was where there was the greatest influx of inotropic drugs. It corresponds to the area where the fluid shed directly from the outlet of the device.

On the other hand, the other irregular area observed corresponded to the parenteral nutrition that shed from the medial lumen. As in Figure 17a, there was a central area with less volumetric fraction of blood because it corresponds to the area where the fluid was discharged. However, Figure 17b shows this region with a greater extension and a lower blood volume fraction compared to Figure 17a; as a result, in the first simulation, the drug velocity of the proximal lumen took a higher velocity, which translates into the insertion of a greater volume of inotropic drug. In Figure 17a, two of the lumens contained blood while the other did not. The lumen which did not contain blood, and was therefore full of fluid therapy, was lumen 1, which did not have any section of lumen below the hole and had an outlet at the end of the catheter. In Figure 17b, on the other hand, two lumens did not contain blood while one did. The justification for the distal lumen was the same as in the case mentioned above: in this lumen, fluid therapy circulated exclusively. Finally, and unlike Figure 17a, the proximal lumen did not contain blood. This indicated that the analysed diametrical cut was at the height of the stream composed only of inotropic drugs.

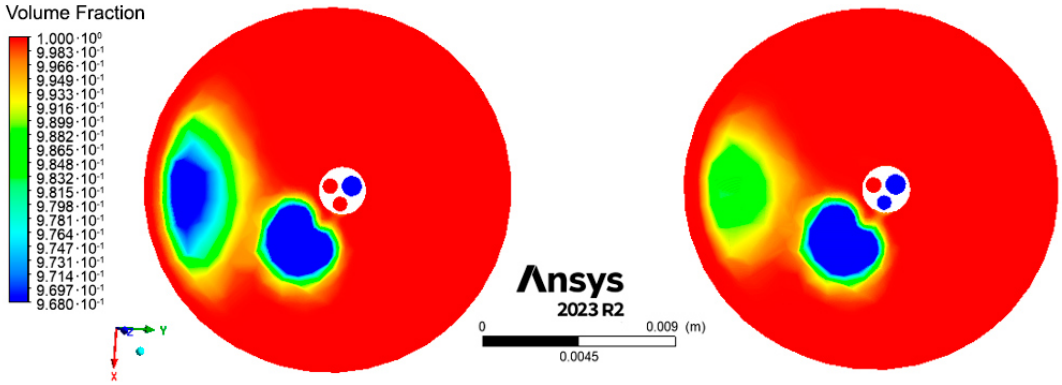

Figure 17. Contours of volumetric fraction of blood in a diametric section of the brachiocephalic trunk. (**a**) Inotropic drug flow rate of 35 mL/h, (**b**) inotropic drug flow rate of 15 mL/h.

Figure 18 represents the path of parenteral nutrition particles from the medial lumen to the end of the vena cava. In both cases, it was observed how the fluid left the medial lumen in the final direction of the lumen, and then joined the bloodstream following the direction of the blood. The trajectory described was almost parallel to the wall of the venous tube. In both figures, it can be seen how the fluid bifurcated approximately halfway through the journey. In Figure 18a, which corresponds to the simulation with the highest inlet velocity into lumen 3, nutrition was divided later, that is, when the particles travelled the longest. In Figure 18b, on the other hand, it was observed that the particles split their trajectory before the middle of the journey. Therefore, it could be concluded that the faster the particles of the blood environment move, the less noticeable was the branching of fluid that occurred in the medial lumen.

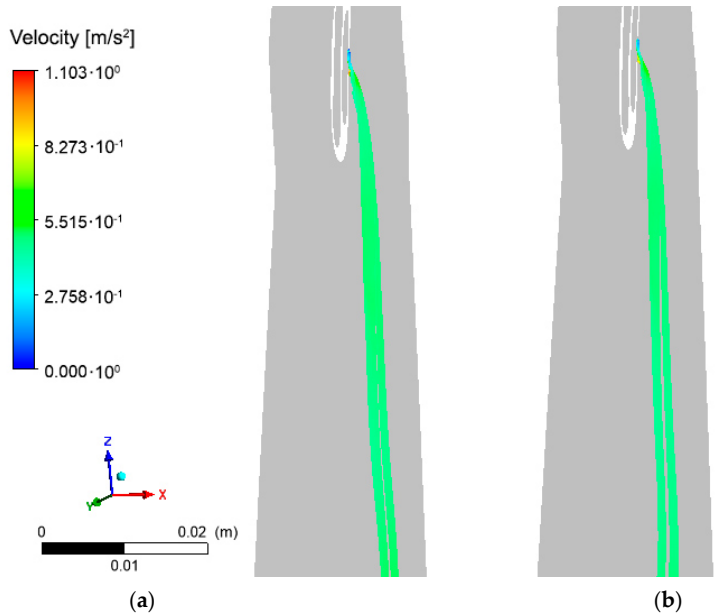

Figure 18. Contours of volumetric fraction of parental nutrition from the medial lumen to the end of the vena cava. (**a**) Inotropic drug flow rate of 35 mL/h, (**b**) inotropic drug flow rate of 15 mL/h.

3.2.3. Mixture Quality Study

Table 10 presents the percentages of the quality of mixture produced between the blood and the various insertion fluids in a sectional cut in the brachiocephalic trunk, close to the last distal lumen of the catheter, and in a sectional cut at the exit of the vena cava. In general, it can be concluded that in the four simulations, the percentages of the quality of

the mixture indicated that a homogeneous mixture was produced between the fluid and the blood. In the sectional section of the vena cava, this value increased with respect to the sectional section in the brachiocephalic trunk, so it could be concluded that the mixture improved slightly as it progressed through the system. However, this change did not occur with significant effects due to the laminarity of the flow. Simulations 1a and 1b presented better percentages than simulations 2a and 2b in both sections. The presence of the fluid inserted in the second lumen decreased the mixing quality.

Table 10. Percentage values of mixture quality in two sectional cuts.

Simulation	Brachiocephalic Trunk Sectional Cut	Lower Vena Cava Sectional Cut
1a. Fluid therapy at constant velocity and inotropic drug at 35 mL/h	62.96%	69.88%
1b. Fluid therapy at constant velocity and inotropic drug at 15 mL/h	68.39%	76.04%
2a. Fluid therapy at constant velocity, inotropic drug dosage from simulation 1.1 is repeated and medial lumen with PTN is added.	54.39%	66.85%
2b. Fluid therapy at constant velocity, inotropic drug dosage from simulation 1.2 is repeated and medial lumen with PTN is added.	58.09%	66.27%

The insertion speed also had significant effects on this value. Thus, if simulations 1a and 1b are compared, it could be observed that the mixture occurred more effectively when the insertion velocity of the inotropic drug was lower. In simulation 2a and 2b, no significant changes were observed in the sectional cut of the vena cava, but they were observed in the cut in the brachiocephalic venous trunk, where the same pattern as in simulations 1a and 1b was observed. Therefore, it could be pointed out that simulation 1b, which involved the operation of two lumens and the insertion of the inotropic drug at low speed, obtained the best mixing quality. On the other hand, the simulation in which the quality of the mixture became lower was obtained in the presence of three lumens.

From these two observations, it could be considered that the reduction of the lumens and a low velocity of the inserted fluid favours the quality of the mixture as they reduced the effort required for intermingling.

4. Conclusions

In this work, two objectives were considered: to study the effect of the insertion of a catheter on the fluid dynamic properties of the blood flow and to study the homogeneity of the mixture of blood and medical fluids infused through this device, produced at the end of the venous structure considered. This study produced the following observations:

- The insertion of the catheter contributes to the minimization of fluid-tight blood areas.
- The variation in blood velocity has no significant effects on the distribution of blood throughout the system. The phenomena of vorticities, fluid-tight zones and irregular distributions remain undifferentiated at both blood velocities, although it can be noted that the reduction in velocity implies a lower Reynolds number and therefore a slight increase in blood laminarity.
- The presence of the fluid infused in the medial lumen has no significant effects on the trajectory of the fluids infused in the proximal and distal lumen. However, changes are observed in the distribution of the final blood mixture and more extensive confluence zones of the three fluids are created.
- The design of the catheter causes a volume of blood to be in a stagnant state for a period of time inside the lumens, which can produce negative consequences due to the biological nature of the fluid.

- Considering the results of the quality of the mixture, a remarkable homogeneity in all simulations that increases slightly as it moves through the system occurs. Although it is a fluid in the laminar regime, the changes do not have significant effects. This observation, therefore, verifies the second hypothesis, that proposes the homogenization of the mixture in the venous area before its entrance to the heart. The system with the highest quality values corresponds to the simulation in the presence of fewer infused fluids and at low speed.

Future work may focus on improvements of this work and further analysis. Regarding the improvements, the distensibility of the veins can be considered as well as non-regular cylindrical shapes. Also, the blood models used should be improved by considering a multiphase or particulate model for the blood and a non-linear model for the viscosity.

Regarding further analysis, different placements of the catheter as well as the lumen outlets can be considered. From the point of view of components (blood and drugs), the interaction between them in physical terms as well as biological may be considered (for instance, the presence of stagnant blood inside the lumens).

Author Contributions: Conceptualization, C.T. and J.V.-C.; methodology, C.T. and J.V.-C.; validation, C.T., J.V.-C., L.H.-C. and M.U.-R.; formal analysis, C.T., J.V.-C., L.H.-C. and M.U.-R.; investigation, L.H.-C., M.U.-R., C.T. and J.V.-C.; data curation, C.T., J.V.-C., L.H.-C. and M.U.-R.; writing—original draft preparation, L.H.-C. and M.U.-R.; writing—review and editing, C.T., J.V.-C., L.H.-C. and M.U.-R.; visualization, C.T., J.V.-C., L.H.-C. and M.U.-R.; supervision, C.T. and J.V.-C. All authors have read and agreed to the published version of the manuscript.

Funding: This research received no external funding.

Acknowledgments: We appreciate the collaboration and help of the entire team of professionals from the Intensive Care Unit of the Arnau University Hospital in Vilanova de Lleida in the compilation of information and obtaining data through the provided images of vascular ultrasound and echo-doppler, essential for the experimental part of the study. We also want to make a special mention of the nurse Blai Rubinat who has contributed to the project by contributing his related knowledge in the health field. We are grateful to Jordi Pallarés Curto (Department of Mechanical Engineering, Universitat Rovira i Virgili) for checking the manuscript and giving advice to the authors.

Conflicts of Interest: The authors declare no conflicts of interest.

Nomenclature

CFD	Computational Fluid Dynamics
CVCT	Tunnelled Central Venous Catheter
FIS	Fluid-Structure Interaction
ICA	Internal Carotid Artery
MRI	Magnetic Resonance Imaging
NTP	Nutrition Total Parenteral
OSI	Oscillatory Shear Index
PICC	Peripherally Inserted Central Catheter
Re	Reynolds number
RVS	Subcutaneous Venous Reservoir
TBAD	Descending Thoracic Aorta
We	Weber number
WSS	Wall Shear Stress

References

1. Sistema Circulatorio: Función, Órganos y Enfermedades. Available online: https://www.healthline.com/health/es/sistema-circulatorio (accessed on 19 July 2024).
2. Definición de Vaso Sanguíneo—Diccionario de Cáncer del NCI—NCI. Available online: https://www.cancer.gov/espanol/publicaciones/diccionarios/diccionario-cancer/def/vaso-sanguineo (accessed on 19 July 2024).

3. Hall, J.E.; Casanova, X.C.; Beltran, N.C.; del Cerro, D.S. *Guyton & Hall. Tratado de Fisiología Médica*, 14th ed.; Elsevier: Amsterdam, The Netherlands, 2021; ISBN 978-84-13-82013-2.
4. Sangre. Available online: https://medlineplus.gov/spanish/blood.html (accessed on 19 July 2024).
5. Julia Reiriz Palacios Sangre. Available online: https://www.infermeravirtual.com/files/media/file/102/Sangre.pdf?1358605574 (accessed on 19 July 2024).
6. El Catéter Central de Inserción Periférica (PICC) se Recomienda Como Sistema de Acceso Venoso en los Pacientes con Tratamiento Oncológico. Available online: https://www.oncoavanze.es/news/el-cateter-central-de-insercion-periferica-se-recomienda-como-sistema-de-acceso-venoso-en-los-pacientes-con-tratamiento-oncologico/ (accessed on 19 July 2024).
7. Definición de Catéter Central de Acceso Venoso—Diccionario de Cáncer del NCI—NCI. Available online: https://www.cancer.gov/espanol/publicaciones/diccionarios/diccionario-cancer/def/cateter-central-de-acceso-venoso (accessed on 19 July 2024).
8. Información Sobre el Catéter Central de Inserción Periférica (PICC) | Memorial Sloan Kettering Cancer Center. Available online: https://www.mskcc.org/es/cancer-care/patient-education/about-your-peripherally-inserted-central-catheter-picc (accessed on 19 July 2024).
9. Pukkas Catéteres Venosos Centrales. Available online: https://fcarreras.org/blog/cvc/ (accessed on 19 July 2024).
10. Catéteres Tunelizados para Hemodiálisis. Available online: https://www.nefrologiaaldia.org/es-articulo-cateteres-tunelizados-hemodialisis-427 (accessed on 19 July 2024).
11. Paola Paolinelli, G. Principios físicos e indicaciones clínicas del ultrasonido doppler. *Rev. Med. Clin. Condes* **2013**, *24*, 139–148. [CrossRef]
12. Fox, R.W.; Pritchard, P.J.; McDonald, A.T. *Introduction to Fluid Mechanics*; John Wiley & Sons: Hoboken, NJ, USA, 2010; ISBN 978-0-470-54755-7.
13. Reynolds' Number—An Overview | ScienceDirect Topics. Available online: https://www.sciencedirect.com/topics/engineering/reynolds-number (accessed on 19 July 2024).
14. OpenStax 12.1 Flow Rate and Its Relation to Velocity. 2016. Available online: https://openstax.org/books/college-physics-2e/pages/12-1-flow-rate-and-its-relation-to-velocity (accessed on 19 July 2024).
15. Hu, H.H. Chapter 10—Computational Fluid Dynamics. In *Fluid Mechanics*, 5th ed.; Kundu, P.K., Cohen, I.M., Dowling, D.R., Eds.; Academic Press: Boston, MA, USA, 2012; pp. 421–472, ISBN 978-0-12-382100-3.
16. Lorenzini, G. Numerical Study of the Flow Disturbance Caused by an Intravascular Doppler Catheter in a Blood Vessel. In *Advances in Fluid Mechanics*; WIT Press: Southampton, UK, 1998; Volume 21, p. 112.
17. Krams, R.; Wentzel, J.J.; Cespedes, I.; Vinke, R.; Carlier, S.; Van Der Steen, A.F.W.; Lancee, C.T.; Slager, C.J. Effect of Catheter Placement on 3-D Velocity Profiles in Curved Tubes Resembling the Human Coronary System. *Ultrasound Med. Biol.* **1999**, *25*, 803–810. [CrossRef] [PubMed]
18. Manos, T.A.; Sokolis, D.P.; Giagini, A.T.; Davos, C.H.; Kakisis, J.D.; Stergiopulos, N.; Karayannacos, P.E.; Tsangaris, S. Local Hemodynamics and Intimal Hyperplasia at the Venous Side of Porcine Carotid Artery—Jugular Vein Shunt. In Proceedings of the 2008 8th IEEE International Conference on BioInformatics and BioEngineering, Athens, Greece, 8–10 October 2008.
19. Soleimani, S.; Pennati, G.; Dubini, G. Numerical Simulation of Thrombus Aspiration Catheter: Preliminary Results. In Proceedings of the 8th International Conference on Advancements of Medicine and Health Care through Technology, Cluj-Napoca, Romania, 29 August–2 September 2011; Volume 36, pp. 256–259.
20. Piper, R.; Carr, P.J.; Kelsey, L.J.; Bulmer, A.C.; Keogh, S.; Doyle, B.J. The Mechanistic Causes of Peripheral Intravenous Catheter Failure Based on a Parametric Computational Study. *Sci. Rep.* **2018**, *8*, 3441. [CrossRef] [PubMed]
21. Weber, P.W.; Coursey, C.A.; Howle, L.E.; Nelson, R.C.; Nichols, E.B.; Schindera, S.T. Modifying Peripheral IV Catheters with Side Holes and Side Slits Results in Favorable Changes in Fluid Dynamic Properties during the Injection of Iodinated Contrast Material. *Am. J. Roentgenol.* **2009**, *193*, 970–977. [CrossRef]
22. Lopes, D.; Puga, H.; Teixeira, J.C.; Teixeira, S.F. Influence of Arterial Mechanical Properties on Carotid Blood Flow: Comparison of CFD and FSI Studies. *Int. J. Mech. Sci.* **2019**, *160*, 209–218. [CrossRef]
23. Chen, Z.; Zheng, Q.; Tong, Z.; Huang, X.; Yu, A. Numerical Modelling of the Interaction between Dialysis Catheter, Vascular Vessel and Blood Considering Elastic Structural Deformation. *Int. J. Numer. Methods Biomed. Eng.* **2024**, *40*, e3811. [CrossRef]
24. Jin, Z.-H.; Barzegar Gerdroodbary, M.; Valipour, P.; Faraji, M.; Abu-Hamdeh, N.H. CFD Investigations of the Blood Hemodynamic inside Internal Cerebral Aneurysm (ICA) in the Existence of Coiling Embolism. *Alex. Eng. J.* **2023**, *66*, 797–809. [CrossRef]
25. Chandran, K.; Dalal, I.S.; Tatsumi, K.; Muralidhar, K. Numerical Simulation of Blood Flow Modeled as a Fluid- Particulate Mixture. *J. Non-Newton. Fluid Mech.* **2020**, *285*, 104383. [CrossRef]
26. Hosseini, S.M.; Feng, J.J. A Particle-Based Model for the Transport of Erythrocytes in Capillaries. *Chem. Eng. Sci.* **2009**, *64*, 4488–4497. [CrossRef]
27. Phillips, R.J.; Armstrong, R.C.; Brown, R.A.; Graham, A.L.; Abbott, J.R. A Constitutive Equation for Concentrated Suspensions That Accounts for Shear-induced Particle Migration. *Phys. Fluids A Fluid Dyn.* **1992**, *4*, 30–40. [CrossRef]
28. Sharan, M.; Popel, A.S. A Two-phase Model for Flow of Blood in Narrow Tubes with Increased Effective Viscosity near the Wall. *Biorheology* **2001**, *38*, 415–428. [PubMed]

29. Qiao, Y.; Zeng, Y.; Ding, Y.; Fan, J.; Luo, K.; Zhu, T. Numerical Simulation of Two-Phase Non-Newtonian Blood Flow with Fluid-Structure Interaction in Aortic Dissection. *Comput. Methods Biomech. Biomed. Eng.* **2019**, *22*, 620–630. [CrossRef] [PubMed]
30. Stamou, A.C.; Radulovic, J.; Buick, J.M. A Comparison of Newtonian and Non-Newtonian Models for Simulating Stenosis Development at the Bifurcation of the Carotid Artery. *Fluids* **2023**, *8*, 282. [CrossRef]
31. Apostolidis, A.J.; Beris, A.N. Modeling of the Blood Rheology in Steady-State Shear Flows. *J. Rheol.* **2014**, *58*, 607–633. [CrossRef]
32. Ivanova, Y.; Yukhnev, A.; Tikhomolova, L.; Smirnov, E.; Vrabiy, A.; Suprunovich, A.; Morozov, A.; Khubulava, G.; Vavilov, V. Experience of Patient-Specific CFD Simulation of Blood Flow in Proximal Anastomosis for Femoral-Popliteal Bypass. *Fluids* **2022**, *7*, 314. [CrossRef]
33. Ansys | Engineering Simulation Software. Available online: https://www.ansys.com/ (accessed on 21 July 2024).
34. Murphy, J.G.; Rajagopal, K.R. The Residually Stressed Unloaded State of Arteries: Membrane and Thin Cylinder Approximations. *J. Mech. Behav. Biomed. Mater.* **2021**, *122*, 104521. [CrossRef]
35. Secomb, T.W. Hemodynamics. *Compr. Physiol.* **2016**, *6*, 975–1003. [CrossRef]
36. Takahashi, T.; Shintani, Y.; Murayama, R.; Noguchi, H.; Rn, M.A.-D.; Koudounas, S.; Rn, G.N.; Mori, T.; Sanada, H. Ultrasonographic Measurement of Blood Flow of Peripheral Vein in the Upper Limb of Healthy Participants: A Pilot Study. *J. Jpn. Soc. Wound Ostomy Cont. Manag.* **2021**, *25*, 576–584.
37. Velocity of Blood Flow in Normal Human Venae Cavae | Circulation Research. Available online: https://www.ahajournals.org/doi/10.1161/01.RES.23.3.349 (accessed on 19 July 2024).
38. Foor, J.S.; Moureau, N.L.; Gibbons, D.; Gibson, S.M. Investigative Study of Hemodilution Ratio: 4Vs for Vein Diameter, Valve, Velocity, and Volumetric Blood Flow as Factors for Optimal Forearm Vein Selection for Intravenous Infusion. *J. Vasc. Access* **2024**, *25*, 140–148. [CrossRef]
39. Hoffmann, O.; Weih, M.; von Münster, T.; Schreiber, S.; Einhäupl, K.M.; Valdueza, J.M. Blood Flow Velocities in the Vertebral Veins of Healthy Subjects: A Duplex Sonographic Study. *J. Neuroimaging* **1999**, *9*, 198–200. [CrossRef]
40. Thomas, B.; Sumam, K.S. Blood Flow in Human Arterial System-A Review. *Procedia Technol.* **2016**, *24*, 339–346. [CrossRef]
41. Jing, T.; Cheng, Y.; Wang, F.; Bao, W.; Zhou, L. Numerical Investigation of Centrifugal Blood Pump Cavitation Characteristics with Variable Speed. *Processes* **2020**, *8*, 293. [CrossRef]
42. Nogourani, Z.S.; Alizadeh, A.; Salman, H.M.J.; Al-Musawi, T.; Pasha, P.; Waqas, M.; Ganji, D.D. Numerical Investigation of the Effect of Changes in Blood Viscosity on Parameters Hemodynamic Blood Flow in the Left Coronary Artery with Consideration Capturing Fluid–Solid Interaction. *Alex. Eng. J.* **2023**, *77*, 369–381. [CrossRef]
43. García-Callejo, F.J.; Balaguer-García, R.; Lis-Sancerni, M.D.; Ruescas-Gómez, L.; Murcia-López, M. Blood Viscosity in COVID-19 Patients With Sudden Deafness. *Acta Otorrinolaringol. Engl. Ed.* **2022**, *73*, 104–112. [CrossRef]
44. Torras, C.; Pallares, J.; Garcia-Valls, R.; Jaffrin, M.Y. Numerical Simulation of the Flow in a Rotating Disk Filtration Module. *Desalination* **2009**, *235*, 122–138. [CrossRef]
45. Netter. Atlas de Anatomía Humana. Abordaje Regional—9788413823980. Available online: https://tienda.elsevier.es/netter-atlas-de-anatomia-humana-abordaje-regional-9788413823980.html (accessed on 19 August 2024).
46. ¿Qué es Tronco Venoso Braquiocefálico? Diccionario Médico. Clínica U. Navarra. Available online: https://www.cun.es/diccionario-medico/terminos/tronco-venoso-braquiocefalico (accessed on 19 July 2024).
47. Mahler, S.A.; Massey, G.; Meskill, L.; Wang, H.; Arnold, T.C. Can We Make the Basilic Vein Larger? Maneuvers to Facilitate Ultrasound Guided Peripheral Intravenous Access: A Prospective Cross-Sectional Study. *Int. J. Emerg. Med.* **2011**, *4*, 53. [CrossRef]
48. Irfan, H.; Ooi, G.S.; Kyin, M.M.; Ho, P. Revealing Maximal Diameter of Upper Limb Superficial Vein with an Elevated Environmental Temperature. *Int. J. Chronic Dis.* **2016**, *2016*, 8096473. [CrossRef]
49. Tiwari, N.; Budhathoki, D.; Shrestha, I.; Timsina, R.; Shah, S.K.; Malla, B.K. Morphology of Dorsal Venous Arch of Hand: A Cadaveric Study. *J. Coll. Med. Sci.-Nepal* **2019**, *15*, 139–143. [CrossRef]
50. Salari, M.; Sasani, M.R.; Masjedi, M.; Pourali, A.; Aghazadeh, S. The Association of Diameter and Depth of Internal Jugular and Subclavian Veins with Hand Dominancy. *Electron. Physician* **2018**, *10*, 7115–7119. [CrossRef]
51. Zhu, P.; Zhang, X.; Luan, H.; Feng, J.; Cui, J.; Wu, Y.; Zhao, Z. Ultrasonographic Measurement of the Subclavian Vein Diameter for Assessment of Intravascular Volume Status in Patients Undergoing Gastrointestinal Surgery: Comparison with Central Venous Pressure. *J. Surg. Res.* **2015**, *196*, 102–106. [CrossRef]
52. Bano, S.; Qadeer, A.; Akhtar, A.; ur-Rehman, H.M.A.; Munawar, K.; Hussain, S.W.; Khan, M.T.; Zafar, R.; Bano, S.; Qadeer, A.; et al. Measurement of Internal Jugular Vein and Common Carotid Artery Diameter Ratio by Ultrasound to Estimate Central Venous Pressure. *Cureus* **2018**, *10*, e2277. [CrossRef]
53. Tartière, D.; Seguin, P.; Juhel, C.; Laviolle, B.; Mallédant, Y. Estimation of the Diameter and Cross-Sectional Area of the Internal Jugular Veins in Adult Patients. *Crit. Care* **2009**, *13*, R197. [CrossRef]
54. Anatomical Study of the Coexistence of the Postaortic Left Brachiocephalic Vein with the Postaortic Left Renal Vein with a Review of the Literature. Available online: https://www.jstage.jst.go.jp/article/ofaj/91/3/91_73/_article/-char/en (accessed on 19 July 2024).
55. ImageJ. Available online: https://imagej.net/ij/index.html (accessed on 19 July 2024).

56. Skewness Calculation in Finite Element Analysis. Available online: https://www.engmorph.com/skewness-finite-elemnt (accessed on 19 July 2024).
57. Petrock, S. Is This a Good FEA Mesh? Here's How to Answer Yes, No, and All-You-Need-to-Know About Meshing Infographic. Available online: https://blogs.solidworks.com/tech/2017/08/good-fea-mesh-heres-answer-yes-no-need-know-meshing-infographic.html (accessed on 19 July 2024).